THESIS

DEVELOPMENT OF A LOW-FIREPOWER CONTINUOUS FEED BIOMASS COMBUSTOR

Submitted by

Mars Rayno

Department of Mechanical Engineering

In partial fulfillment of the requirements

For the Degree of Master of Science

Colorado State University

Fort Collins, Colorado

Spring 2020

Master's Committee:

Advisor: Bret Windom
Co-Advisor: John Mizia

Ellison Carter

Copyright by Mars A. Rayno 2020

All Rights Reserved

ABSTRACT

DEVELOPMENT OF A LOW-FIREPOWER CONTINUOUS FEED BIOMASS COMBUSTOR

Approximately 25% of world's population lacks basic sanitation amenities. This lack of sanitation leads directly to the spread of contagious diseases and parasites. One method that can help mitigate these consequences is the thermal treatment of human feces in a combustion system.

Colorado State University's Advanced Biomass Combustion Lab has been working on thermal treatment systems as part of the Bill and Melinda Gates Foundation Reinvent the toilet challenge for over 7 years. The goal is to develop stand-alone treatment technologies that can process waste for less than 5 cents per person per day. Thermal processing is an attractive solution because it not only destroys pathogens, but also significantly reduces the amount of mass that needs to be disposed of.

Until recently, the focus has been on larger (2 kW) fecal gasifiers. This scale of combustor was designed to incinerate the solid waste of approximately 28 users per hour. The large amount of users required to operate meant that either fuel would need to be stored before usage or the combustor would be subject to frequent startups and shutdowns. During steady state operation the gasifier emits low quantities of harmful pollutants, but during startup and shutdown the emissions are considerably higher. Thus, there is a need to mitigate or reduce the frequency of those transient events. One way to address this problem is to develop a suite of scaled combustors.

A 500 W combustor, for example, would be able to run continuously for 12 hours with 30 users, or 24 hours with 60 users. This project investigated a scaled version of the 2kW fecal combustor developed under the BMGF RTTC.

Emission factors for this scaled device were generated for various firepowers, air-fuel ratios, and primary-to-secondary air ratios.

ACKNOWLEDGEMENTS

I'd like to thank my advisor, John Mizia, for hiring me in the first place. Generally speaking, I'd disliked thermosciences as an undergrad, but after working for him, I developed a significant interest in combustion science, which suddenly made all the thermosciences work I'd disliked in the past make sense. I'd also like to thank my committee members, Dr. Bret Windom and Dr. Ellison Carter, for their time and expertise.

There are many people at the Colorado State University Powerhouse who helped my work immensely. Thanks are due to Matt Willman and Jason Golly, who helped with all my fabrication needs, and to James Tillotson and Mark James, who assisted me with the 5-Gas data acquisition. Dr. Christian L'Orange was invaluable due to his knowledge of particulate matter data collection and measurements. Iman Babazadeh found my auger on a scrap pile on campus, which actually worked very well for what I needed. Max Flagge answered all my combustion questions when I first started.

I'd also like to express my love and adoration to my wife, Jenny, for supporting me during my Master's work (and for watching the kids while I finished up my thesis at home after COVID-19 struck).

To my daughters, Lily and Claire, may you both one day grow up to be engineers. Math is fun!

TABLE OF CONTENTS

LIST OF TABLES

LIST OF FIGURES

Chapter 1

Introduction

1.1 Problem Statement

The world currently has a population of approximately 7.7 billion people; of these, some 2 billion still lack basic sanitation amenities, such as toilets or latrines [6]. A larger focus on proper sanitation is desperately needed in many developing countries, as poor sanitation is a primary cause for the spread of diseases such as cholera, dysentery, and polio. The global disease burden from different diseases caused by substandard water, sanitation, and the poor hygiene that arises from those amounts to some 1.6 million deaths, representing 2.8% of all annual deaths [7]. 297,000 of those deaths are due to diarrhea in children under 5, some 5.3% of all deaths in that age group [6,7].

Various efforts have been made over the years to address this issue, such as the Sustainable Development Goal by the United Nations and the Reinvent the Toilet Challenge (RTTC), started by the Bill & Melinda Gates Foundation in 2011 [8]. In both of these programs, safe management or elimination of human waste were listed as high priorities to address spread of disease and contamination of drinking water. Cost being a problem for proper sanitation methods in developing countries, the RTTC required that can process waste for less than 5 cents per person per day.

Thermal processing is an attractive solution because it not only destroys pathogens, but also significantly reduces the amount of mass that needs to be disposed of. To that end, incineration of fecal matter has been the primary method by which Colorado State University (CSU) has used to work with the RTTC for over 7 years. Combustion, however, has its own challenges, one of which is that harmful emissions such as carbon monoxide and particulate matter must be accounted for and reduced as much as possible.

1.2 Background

Research Triangle Institute (RTI) was among the participants in the RTTC. Their goal was to develop a reinvented toilet system that operated completely off-grid, with no piped-in water, sewer connection, or outside electricity [1].The Advanced Biomass Combustion Lab at CSU was contracted by RTI to design a high-efficiency combustor to sanitize solid waste as part of that system, shown in Figure 1.1.

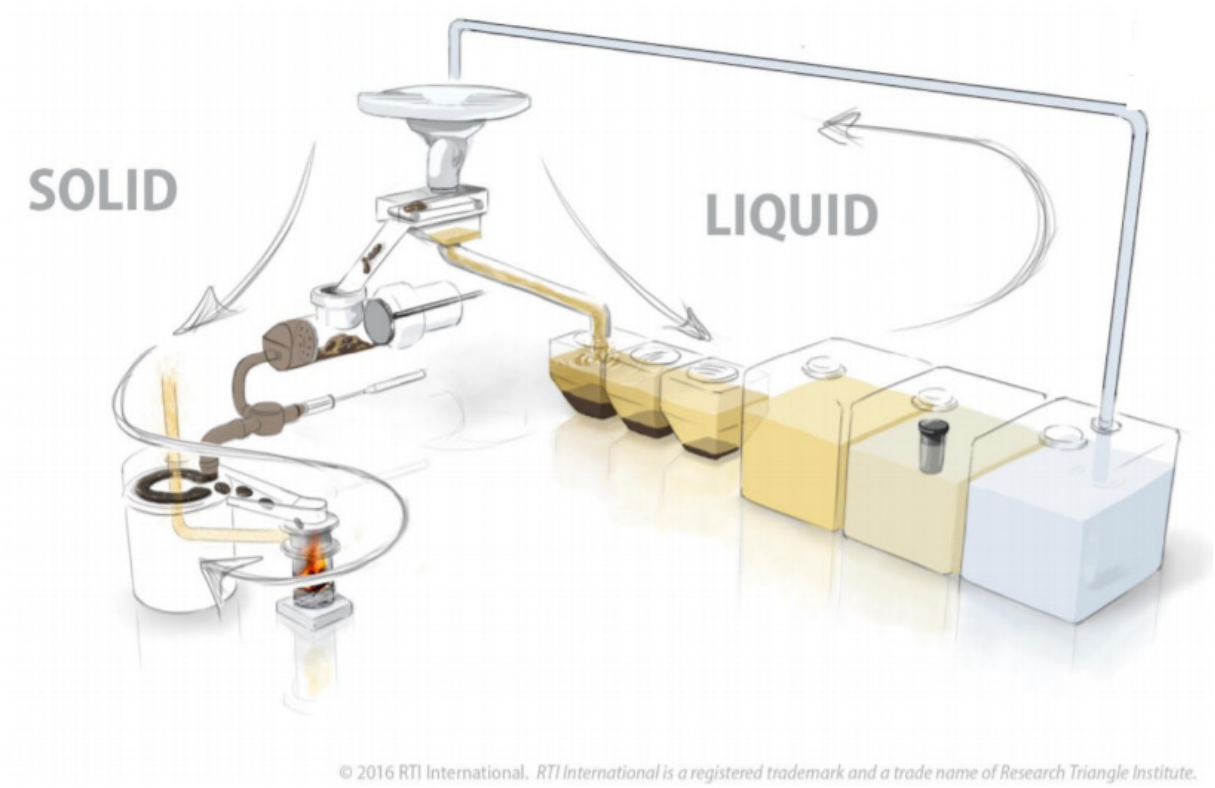

Figure 1.1: Full toilet system proposed by RTI [1].

1.2.1 System Combustors

Downdraft Gasifier

CSU's combustor design centered around a combustor operating as a semi-gasifier, due to gasification's characteristics of low emissions and high combustion efficiency. The original combustor

was a 3.5 kW downdraft gasifier designed by the CSU team; this combustor underwent multiple iterations before a final design was settled upon, shown in Figure 1.2 [2].

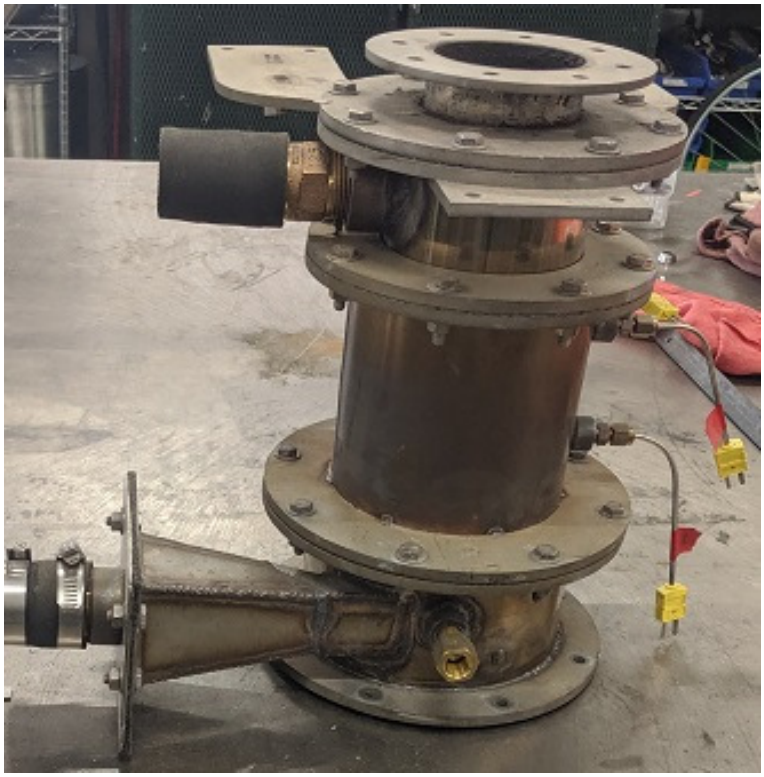

Figure 1.2: Original downdraft gasifier [2].

The combustor's high thermal mass was problematic as it slowed down the achievement of steady state temperatures [2]. Downdraft combustion also required an airlock between the fuel inlet and fuel grate, to prevent hot syngas from flowing up through the unburnt fuel storage as opposed to down through the grate and to the oxidation zone [3]. These main issues meant a new design was called for. This new design planned to simplify the overall combustor, which led to the creation of the micro combustor.

Micro Combustor

The micro combustor was a decrease in mass from 29 kg to only 3 kg. In addition, the micro combustor was switched to an updraft gasification design as it proved to be simpler to control,

with similar emissions [3]. This combustor was designed to operate at 2 kW using dried feces as fuel [3].

Figure 1.3: Updraft gasifier [3].

Additional work led to the V3 micro combustor shown in Figure 1.3, which was used for characterization of the micro combustor design. The V3 was very stable, able to run continuously for 24 hours using wood pellets [3]. However, it was not useful for introduction into the full toilet system, as its small forced air inlets would not function well when controlled by an exhaust fan. This led to a new micro combustor design with a single manifold for both primary and secondary

air inlets. This new "monofold" design, shown in Figure 1.4, is described extensively in Flagge's work and will not be discussed here [3].

Figure 1.4: Updraft gasifier - monofold design [3].

1.3 Scaled Combustor Catalog

Human feces is roughly 74.6% wet, meaning that an average human's deposit of 250 g will only be 38 g when dried [9]. The micro combustor was designed to operate at 2 kW, meaning that for 12 hours of operation it will need 400 g/hr, or about 120 people's feces. The RTI system described would therefore be aimed at servicing a large village.

But what about smaller villages or large households?

Table 1.1: Combustor size scaling for different firepowers and user base.

Firepower $[W]$	Fuel Rate [g/hr]	Burn Duration [hr]	Req. Users [#]
100	20	12	6
100	20	24	12
500	100	12	30
500	100	24	60
1000	200	12	60
1000	200	24	120
2000	400	12	120
2000	400	24	240

The micro combustor, as sized, does not scale down to a lower firepower very effectively due to the requirement of a consistently sized pyrolysis zone. A smaller flame in the micro combustor leads to a smaller pyrolysis zone, making consistent combustion much harder to achieve.

Running the micro combustor at its design size of 2 kW with fewer users means more frequent startups and shutdowns of the system. With some 99% of total emissions occuring during startup/shutdown and refueling events, which encompass only 20% of a burn duration, transient events should be avoided where possible [10].

Another major issue is not in engineering, but societal. People may desire more privacy than sharing a large scale communal toilet, for instance. In developing countries, women may face unwanted sexual remarks and touching to rape and femicide [11]. Having a smaller, household scale toilet system would help to alleviate some of those problems they face on a daily basis.

CSU envisioned a scaling combustor catalog, able to accommodate different population densities, from a single household to different sized communities. This is shown in Table 1.1.

As the micro combustor filled the role of the high powered combustor, CSU proposed a lower firepower (100 W) design that operates on premixed dust combustion. This next combustor, referred to as the Nano-combustor, was designed in conjunction with Mountain Safety Research (MSR) to operate at a firepower an order of magnitude below the micro combustor [4].

Nano-combustor

The Nano-combustor is a dust combustion device; Figure 1.5 shows the Nano-combustor's final iteration.

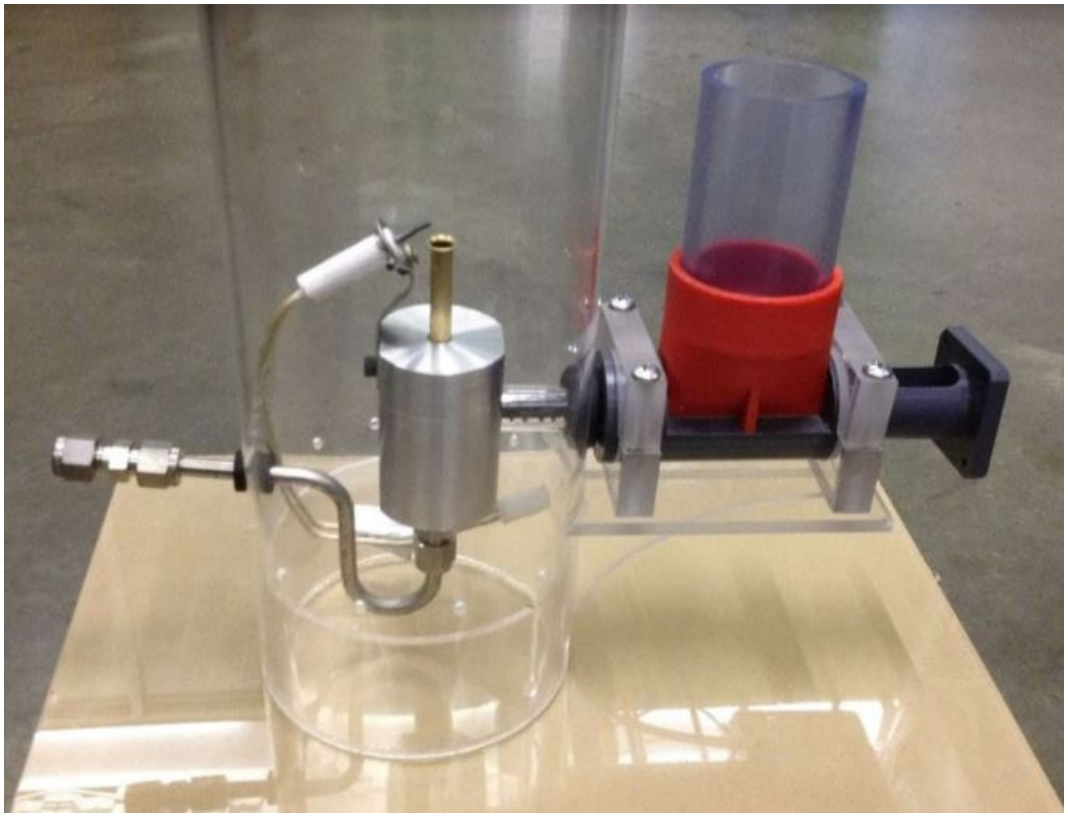

Figure 1.5: Final design of the Nano-combustor [4].

In this design, dust is fed from the 3d printed hopper via auger into a machined aluminum tee. Air is injected at the bottom of this tee, where it mixes with the incoming dust, and is ejected at the top at the brass nozzle. A 12 VDC hot surface igniter located at the exit ignited the fuel-air mixture to produce flame [4].

The Nano-combustor was primarily tested using Lycopodium powder as an idealized fuel during development because of its free-flowing nature and monodisperse particle size distribution [4]. Using this idealized fuel, the Nano-combustor was able to burn in durations greater than 45 minutes at 240 W [12].

While the design of the Nano-combustor was novel, it suffered from serious flame stability issues when using powderized fecal fuel, and the burn duration decreased to around 5 minutes at 500 W [12]. The design began to grow increasingly complex in order to combat the stability problem. In addition, it became obvious that in order to use fecal dust, the dust itself had to undergo energy intensive processing in order to be uniform in size and shape to avoid clumping; as shown in Figure 1.6, simple grinding left many surface defects that tended to cause unwanted agglomeration [4].

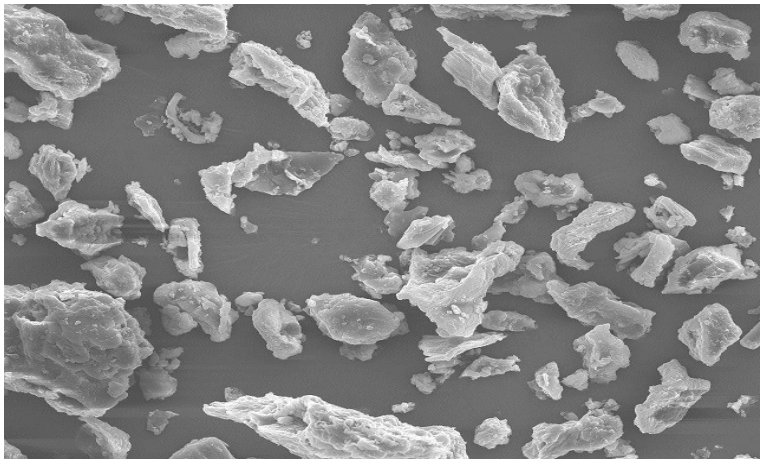

Figure 1.6: Scanning Electron Microscope image of fecal flakes after undergoing simple grinding [4]

1.4 Project Goals & Deliverables - the Micro Mini

Due to the increasing complexity and short burn durations of dust combustion when a continuously burning combustor was desired, the design success of the micro combustor was revisited. The micro combustor works well for a large village, with number of users shown in Table 1.1, but for smaller scale operation such as a smaller village or household the frequent startups and shutdowns produce a large amount of pollutants. An example of high emissions during shutdown is shown in Figure 1.7 using a batch-fed gasifier. Figure 1.7(E) would correspond to the large spike shown in Figure 1.8.

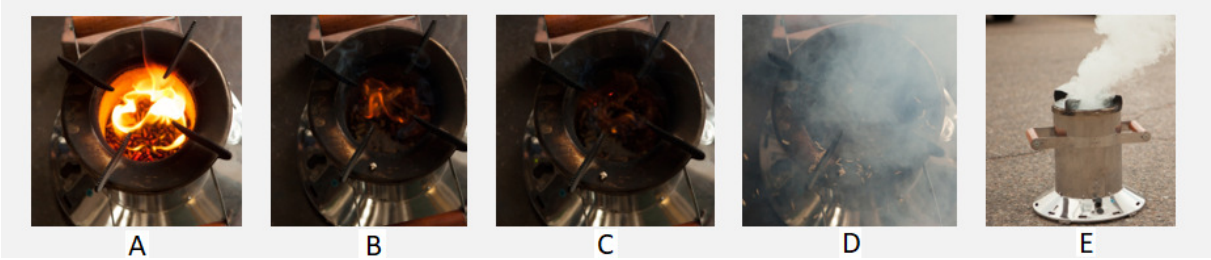

Figure 1.7: Gasifier normal operation (A), low on fuel (B), out of fuel (C), flame out (D) and (E).

A downsized gasifier which utilizes uniform, small, and consistently sized fuel would be able to achieve the lower firepower the larger version cannot match. It would be capable of continuous operation as it consumes less fuel to keep firepower low, reducing the amount of transient event occurence, and be able to prove the efficacy of Table 1.1. Figure 1.8 shows the low emissions achieved by continuous operation, with a large spike showing a short flame out followed by relight.

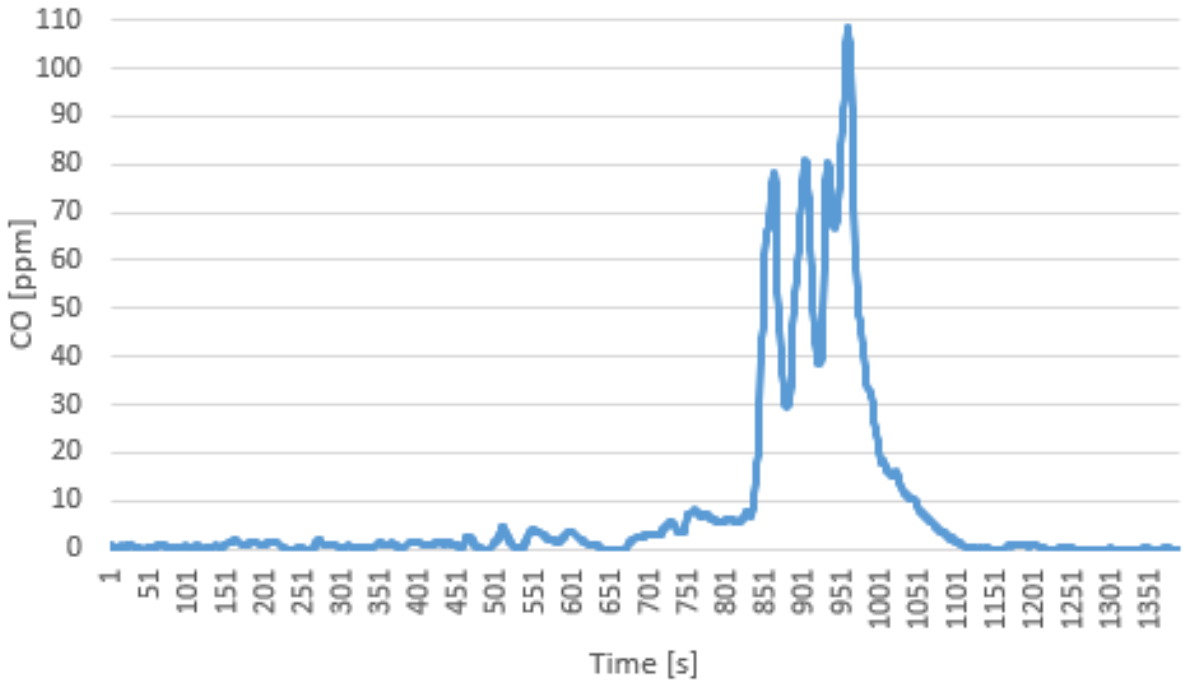

Figure 1.8: Gasifier low emissions during normal operation, with a short flame out followed by relight.

This downsized system would achieve more consistent flames than the Nano-combustor due to the relative ease of feeding and burning solid fuel as opposed to dust. Additional challenges dust

combustion faces over solid fuel are surface effects, where the surface of a dust particle can have different chemical composition from adsorption of compounds from air [13]. Dust particle size and shape can affect its combustion by its ability to loft and suspend, thus affecting concentration; essentially the fuel feed rate of the dust [4].

An early iteration of the micro combustor was used as a base model in order to explore downsizing existing technology to develop a compact, low firepower combustor, henceforth referred to as the micro mini. The micro combustor was designed for a firepower of $\backsim$2 kW. As doubling the diameter of the combustor leads to a quadrupling of firepower, then the opposite is true: halving the diameter will lead to a quartering of firepower, or about 500 W. As such, the micro mini's combustor body is half the size of the micro combustor, with the rest of the assembly scaled accordingly.

The micro mini was capable of achieving the stability the larger combustor enjoys, while simultaneously being capable of operating continuously for long periods of time to avoid transient emission penalties. This also reduced the energy needed for fuel processing, as smaller chips are much less energy intensive to produce than a fine powder, such as that needed by the Nanocombustor.

The micro mini was capable of operating at firepowers from 250 W to 890 W. It was able to operate at air to fuel ratios from stoichiometric down to very fuel lean conditions, which help to reduce harmful emissions such as CO and particulate matter, with air was supplied via mass flow controllers on a compressed air line for the bench type prototype.

The goal of this proposed effort was to showcase a working prototype of a low firepower ($\backsim$600 W) biomass combustor upon conclusion of research, which will reinforce the scaling combustor catalog idea described in Section 1.3. The performance and emissions characteristics of the benchtop prototype were tested and reported upon. Recommendations for future work and design suggestions will follow.

Chapter 2

Theory

2.1 Combustion

Combustion is defined as the chemical process in which substances mix with oxygen to produce heat and light. It is an exothermic chemical reaction, and once enough heat is generated by the process, is self-sustaining as long as the fuel and oxidizer last and the heat loss rate isn't greater than the chemical heat release [14].

2.1.1 Stoichiometry

Stoichiometry is the calculation of chemical reactants undergoing a reaction to form products. For a typical hydrocarbon fuel, the calculation is completed using Equation 2.1.

$$C_{\mathrm{x}}H_{\mathrm{y}} + a(O_2 + 3.76N_2) \rightarrow xCO_2 + \frac{y}{2}H_2O + 3.76N_2 \tag{2.1}$$

In this equation, C_xH_y is a hydrocarbon fuel with x Carbon atoms and y Hydrogen atoms. The variable a, the number of moles of air (O_2 + 3.76 times that amount of N_2) combusted with the hydrocarbon, is defined in Equation 2.2 as

$$a = x + \frac{y}{4} \tag{2.2}$$

Equation 2.3 shows the stoichiometric air-fuel ratio (AFR) is calculated as

$$\begin{aligned}\left(\frac{A}{F}\right)_{\mathrm{stoich}} &= \left(\frac{m_{\mathrm{air}}}{m_{\mathrm{fuel}}}\right)_{\mathrm{stoich}} \\ &= \frac{4.76a}{1}\frac{MW_{\mathrm{air}}}{MW_{\mathrm{fuel}}}\end{aligned} \tag{2.3}$$

with m_{air} being the mass of air, m_{fuel} being mass of fuel, MW_{air} being the molecular weight of air, and MW_{fuel} being the molecular weight of the hydrocarbon fuel. The value a is from Equation 2.2.

When the value is exactly stoichiometric, the hydrocarbon is completely oxidized and, in theory, leads to products of only carbon dioxide (CO_2), water (H_2O), and nitrogen (N_2), which ideally passes through the combustion event without oxidizing into some variant of nitrous oxide (NO_x).

More or less air than necessary can be used in the combustion process, leading to different products of combustion. The equivalence ratio, ϕ, is shown in Equation 2.4. ϕ is used to denote whether more air than needed is used (fuel lean condition, or $\phi < 1$), less air than needed is used (fuel rich condition, or $\phi > 1$), or just the right amount (stoichiometric, or $\phi = 1$).

$$\phi = \frac{(\frac{A}{F})_{\text{stoich}}}{(\frac{A}{F})} = \frac{(\frac{F}{A})}{(\frac{F}{A})_{\text{stoich}}} \tag{2.4}$$

Typically, a combustion event at a fuel lean condition will produce CO_2, H_2O, N_2, and excess O_2 as major species, as there is more oxygen available to oxidize carbon monoxide (CO) into CO_2. Conversely, a combustion event at a fuel rich condition will produce CO_2, H_2O, N_2, CO, and H_2, with the two latter products forming as there is not enough oxygen present for them to be oxidized [14].

2.1.2 Heating Values

The heat of combustion, also known as heating value, is the difference in enthalpy between the reactants and products of the combustion event [14]. The heat of combustion represents the energy released when a compound undergoes the combustion process. The higher heating value (HHV) is the heat of combustion when all the water in the products is in liquid form; the lower heating value (LHV) corresponds to when all the water is in gas phase [14]. As all the water in the products in this research was in gaseous phase, the LHV will be used in subsequent calculations.

2.1.3 Firepower

Firepower is a parameter by which the energy output of a combustion event is characterized; firepower is defined in Equation 2.5.

$$FP = \dot{m}_{\text{fuel}} \cdot LHV \tag{2.5}$$

where FP is the measure of firepower in kW, $\dot{m}_{\text{fuel}}$ is the mass flow rate of fuel in kg/s, and LHV is the lower heating value of the fuel in kJ/kg. Firepower was used to compare various tests in this research as it represents ideal energy produced by combustion.

As firepower was used as a variable for analysis, it needed to be quantified before testing began. Appendix A contains a combustion calculator in Matlab developed by the Advanced Biomass Combustion Lab at CSU. This code was used to calculate firepower for different mass flow rates of fuel.

2.1.4 Limits of Flammability

A flame will only propogate within a range of air-fuel ratios between the *lower* and *upper* limits of flammability. The lower limit is the leanest air-fuel ratio that will allow flame propagation, while the upper limit represents the richest [14]. The lower limit of flammability will be discussed further in Section 8.4.

2.2 Gasification Theory

Gasification is the conversion of any carbonaceous fuel to a gaseous product with a useable heating value [15]. In a gasifier, there are four reaction zones, shown in Figure 2.1.

Solid fuel, in this case biomass, is added at the top of the gasifier and enters the drying zone, where the moisture evaporates. As the fuel dries, it enters the pyrolysis zone, wherein the dried biomass is converted to char, tars, and water vapor.

These products enter the reduction zone, where products of complete combustion (CO_2 and H_2O) are reduced to CO, H_2 and CH_4, the primary components of the resulting synthetic gas,

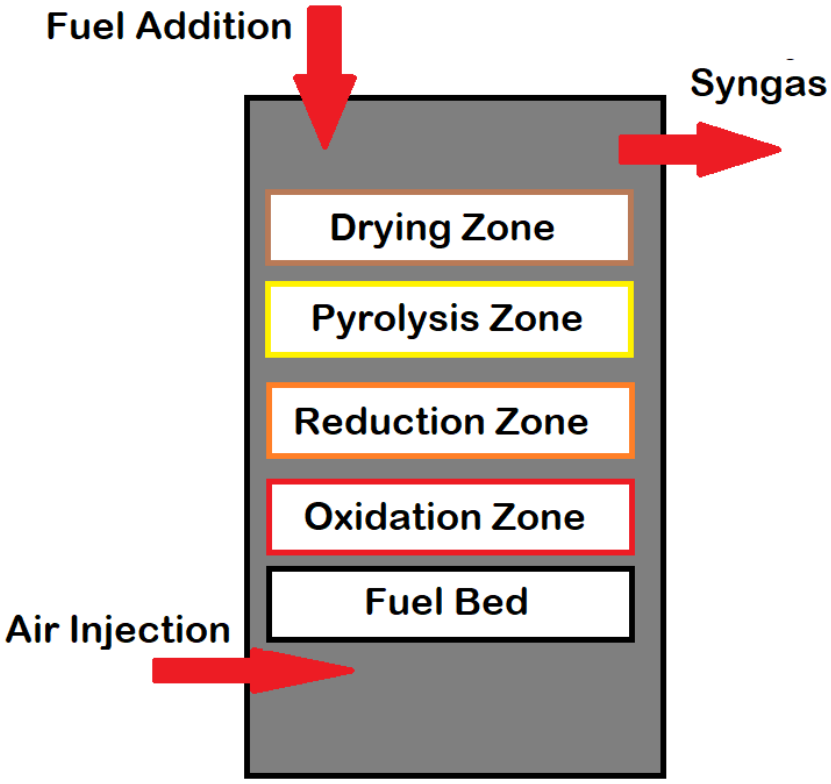

Figure 2.1: Gasifier Processes, shown in an updraft gasifier.

known as "syngas." Syngas constituent compositions can vary somewhat significantly depending on fuel, but is typically 30-60% CO, 25-30% H_2, 0-5% CH_4, and 5-15% CO_2 [16]. Partial oxidation in the oxidation zone occurs by heating the char with a low amount of oxidizer, which releases the heat necessary to drive the processes occurring in the drying, pyrolysis, and reduction zones [17]. The resulting ash then falls below the fuel bed, which is later collected and disposed of.

In a gasifier, the syngas is typically then stored until ready for use. The micro mini is a semi-gasifier; that is, the syngas is combusted downstream of the fuel bed instead of being stored. This secondary combustion occurs at the location of the secondary air injection holes, detailed below in Section 2.2.3. This flame in the secondary combustion zone is referred to as an inverse diffusion flame, which leads to higher temperatures than what occurs at the fuel bed and leads to higher efficiency, which further leads to lower emissions of pollutants.

2.2.1 Gasification Chemistry

The oxidation zone has several important reactions that take place, which produce heat that drive reactions in the other zones, and are shown in Equations 2.6 through 2.8.

$$C + O_2 \rightarrow CO_2 \qquad -394\ MJ/kmol \tag{2.6}$$

$$2CO + O_2 \rightarrow 2CO_2 \qquad -566\ MJ/kmol \tag{2.7}$$

$$2H_2 + O_2 \rightarrow 2H_2O \qquad -484\ MJ/kmol \tag{2.8}$$

The reduction zone is where the complete products of combustion are reduced, shown in Equations 2.9 (the Boudouard reaction) and 2.10 (steam gasification). Equation 2.11 details conversion of Methane.

$$C + CO_2 \rightarrow 2CO \qquad +172\ MJ/kmol \tag{2.9}$$

$$CO + H_2O \rightarrow CO_2 + H_2 \qquad +131\ MJ/kmol \tag{2.10}$$

$$C + 2H_2 \rightarrow CH_4 \qquad -75\ MJ/kmol \tag{2.11}$$

As shown, both Equations 2.9 and 2.10 are endothermic in nature, requiring energy input to react in the forward direction. This energy is easily supplied by the exothermic combustion reactions described in Equations 2.6 through 2.8. Therefore, once ignited, the reactions are continuous.

The syngas, due to its composition, is easily combusted. The reactions for oxidization of syngas are exothermic; that is, they release energy during reaction. Equations 2.12 through 2.14 detail the syngas combustion reactions [15].

$$CO + \frac{1}{2}O_2 = CO_2 \qquad -283\ MJ/kmol \tag{2.12}$$

$$H_2 + \frac{1}{2}O_2 = H_2O \qquad -242\ MJ/kmol \tag{2.13}$$

$$CH_4 + 2O_2 = CO_2 + 2H_2O \qquad -891\ MJ/kmol \tag{2.14}$$

As can be seen, the general products from combustion of syngas tend towards completely oxidized carbon and hydrogen, as discussed in Section 2.1.1.

2.2.2 Types of Gasifiers

There are three main types of gasifiers: downdraft, updraft, and cross-draft. Downdraft and updraft gasification processes were used by CSU researchers during RTTC combustor development, and are discussed below. Cross-draft was not used and will not be described in this report.

Downdraft

In downdraft gasification, fuel is loaded at the top, along with air. The air flows downward through the fuel bed in the drying zone. The partial oxidation that occurs heats the pyrolysis zone, directly beneath it, which also assists in drying the fuel above it. The products from the pyrolysis zone pass through the reduction zone below it, in which CO_2 and H_2O are reduced into the CO and H_2 syngas is primarily composed of. The syngas is then extracted from the bottom, as shown in Figure 2.2.

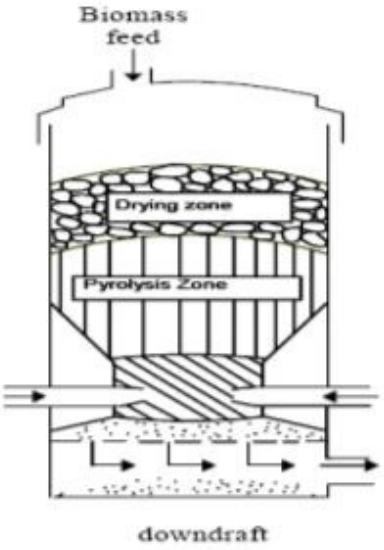

Figure 2.2: Downdraft gasifier design [5]

Updraft

In updraft gasification, fuel is again loaded at the top, but the air is injected at the bottom of the gasifier. The air flows upward through the oxidation zone. The products from the partial oxidation are reduced directly above it, which pyrolyze and dry the incoming fuel. The syngas flowing through the fuel bed is then extracted at the top, as shown in Figure 2.3.

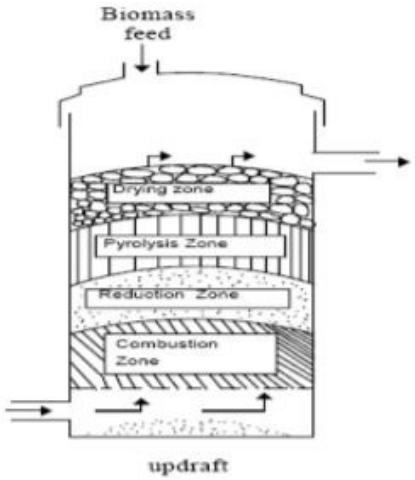

Figure 2.3: Updraft gasifier design [5]

2.2.3 Primary to Secondary Air Flow Ratio

Air flow was introduced in two places in the combustor: just below the fuel bed, called primary air, and downstream from the fuel bed, called secondary air. The primary air is the air that is used in the partial oxidation of the fuel; as such, it must be a lower mass flow overall than the secondary air to discourage complete combustion occurring at the fuel bed.

Studies have shown the ideal primary to secondary mass flow air ratio, for wood biomass, to be 1:4 [18]. Furthermore, higher secondary air velocities have overall lower CO emissions, likely due to a $\phi < 1$ and stronger mixing between secondary air and the syngas [19, 20]. Furthermore, there is a recommended minimum velocity for air injection. As velocity increases, mixing and reaction rate is improved; in general, air velocity exceeding 5 m/s at burner exit is recommended [20].

However, there can be an upper limit on velocity, depending on fuel. Feces, for instance, is significantly less dense than wood, and too much air may lead to lofting of the fuel rather than having it combust in the oxidation zone.

Chapter 3

Combustor Hardware

While both consistent and efficient in operation, the micro combustor is designed for use for a large village. It doesn't work as well for smaller operations. Thus, a combustor sized to work well for smaller scale usage, such as a single household or small grouping of houses, was desired.

Section 1.2 explains why the micro combustor cannot scale down effectively to a lower firepower for a given combustor size due to the requirement of a consistently sized pyrolysis zone. A smaller flame in the micro combustor leads to a smaller pyrolysis zone, making consistent combustion harder to achieve [3]. However, downsizing the micro combustor would take advantage of a proven design, but at a lower firepower.

Initially, the micro combustor "monofold" design described in Section 1.2.1 was chosen as a base for the smaller combustor, as that was the final iteration of micro combustor design. However, combustor characterization required work with many different air injection rates, for both primary and secondary air. The monofold design worked against this, as only one air injection point is available and the different primary and secondary air flows are controlled only by machined air injection holes in the combustor body. Thus, the V3 micro combustor was chosen as a base for the new combustor, as having two separate manifolds would allow for different injection rates at primary and secondary air locations.

As discussed in Section 1.4, halving the combustor body diameter leads to a quartering of expected firepower. As such, the V3's combustor body diameter of 2.5 inches would be halved to 1.25 inches.

3.1 Scaling Calculations

The V3 CAD models were investigated in SolidWorks. As the V3 was due to previous research showing its reliability, the main design was not altered so as to avoid any detrimental effects on performance [3]. Rather, the ratios between the features were scaled using the ratio between the

original combustor body diameter and the new desired diameter and applied to an overall smaller combustor.

To verify that this scaling would prove comparable between the larger micro combustor and the smaller, flame residence time was calculated using Equation 3.1, with ρ being the density of gas, V being the volume of the cylinder, and $\dot{m}$ being the fuel feed rate [14].

$$t_{\mathrm{R}} = \frac{\rho V}{\dot{m}} \tag{3.1}$$

Assuming standard biogas density of 1.15 kg/m^3, Table 3.1 shows that the residence time between the larger combustor and a scaled down version are identical.

Table 3.1: Residence time calculations.

Combustor	Volume [cm^3]	Fuel Rate [g/hr]	Residence Time [s]
Micro	44.2	100	1.83
Micro Mini	176.98	400	1.83

3.2 Fabrication

3.2.1 Main body

Previous combustors, owing to their larger size, were made from rolled stainless steel, having had the general shape and air injection holes water jetted. Due to the smaller size of the micro mini, rolling to that diameter would be much more difficult. For simplicity, the combustor body was made from 1.25 inch 304 stainless steel tube, with a wall thickness of 0.035 inches. This meant that the inner diameter of the micro mini was actually 1.18 inches, 0.07 inches smaller than half the size of the V3 micro combustor.

The initial size scaling calculations called for the body to have a length of 5.9 inches, down from 12 inches of the micro combustor; however, an extra inch was added, with half an inch for

the top and bottom, to allow easier access for welding. This extra half inch at either end did not affect the scaling ratio between primary and secondary air holes.

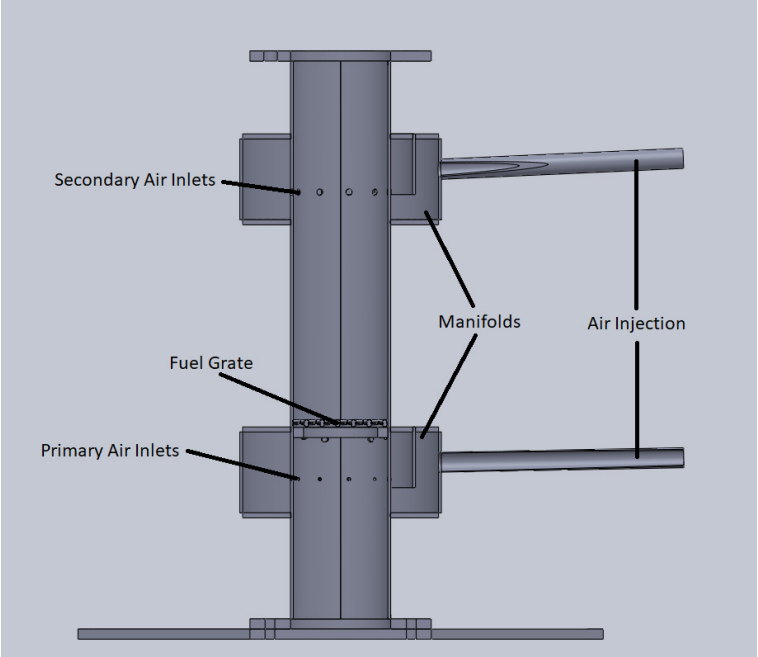

Figure 3.1: Micro mini assembly CAD showing major components.

The two air manifolds were made from 2.5 inch 304 stainless steel tubing, with a wall thickness of 0.035 inches, each 1 inch in height. The tubes for both the combustor body and manifolds were cut to length using a HAAS TL1 CNC Lathe, available at CSU's Rapid Prototyping and Applied Engineering Lab (RPL). Figure 3.1 shows the combustor body and manifold design.

Air injection and fuel grate support holes were machined into the combustor body using a HAAS TMTP2 CNC Mill at the RPL. The 10 primary air injection holes, located just below where the fuel grate would sit, were sized at 1 mm (0.0394 inches). 10 secondary air injection holes were 3.53 inches above the primary air and were sized at 2 mm (0.0787 inches). These sizes were selected to maintain a 1:4 air ratio between the primary and secondary air injection, while keeping the air velocity between them equivalent and above 5 m/s (Section 2.2.3).

The top and bottom collars for the manifolds were cut from 0.035 inch stainless steel using a water jet. The top collar for each manifold also had a U-shape cut into it to allow the addition of a

0.75 inch air deflector, which was added to assist air circulation throughout the manifold. This air deflector is illustrated in Figure 3.2.

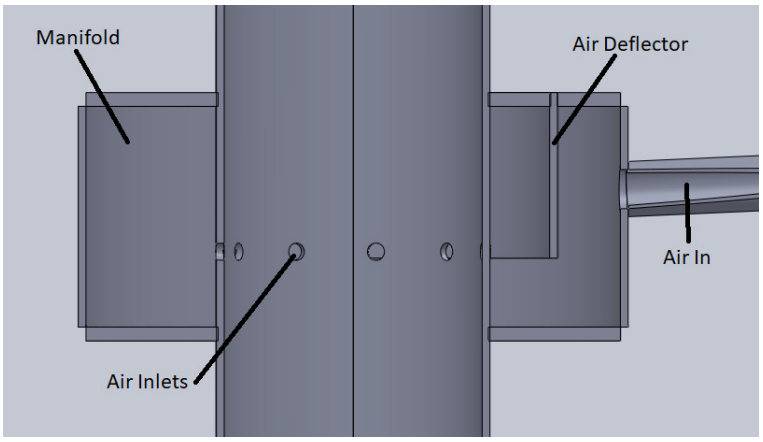

Figure 3.2: Manifold CAD showing air deflector.

The welded micro mini is shown next to the V3 in Figure 3.3.

3.2.2 Fixtures and Secondary Parts

Flanges for mounting were cut from 0.125 inch stainless steel using a water jet. A three legged base was also cut using a water jet, to keep the bottom of the combustor from direct contact with the ground. This allowed air flow underneath the combustor to act as an insulator to keep heat flowing up through the combustor body, as well as acting as a cap to keep the primary air flowing up.

Compressible graphite gaskets, 0.035 inches thick, were used as seals between mounting flanges to prevent any air leakage that would affect air flow. Six M10 sized socket cup bolts were used to connect the flanges between the body, base, and fuel chute (see Section 5.3). The fuel grate material was acid-resistant 400 Nickel wire cloth, which supported the fuel bed while allowing ash to drop through to the bottom of the combustor.

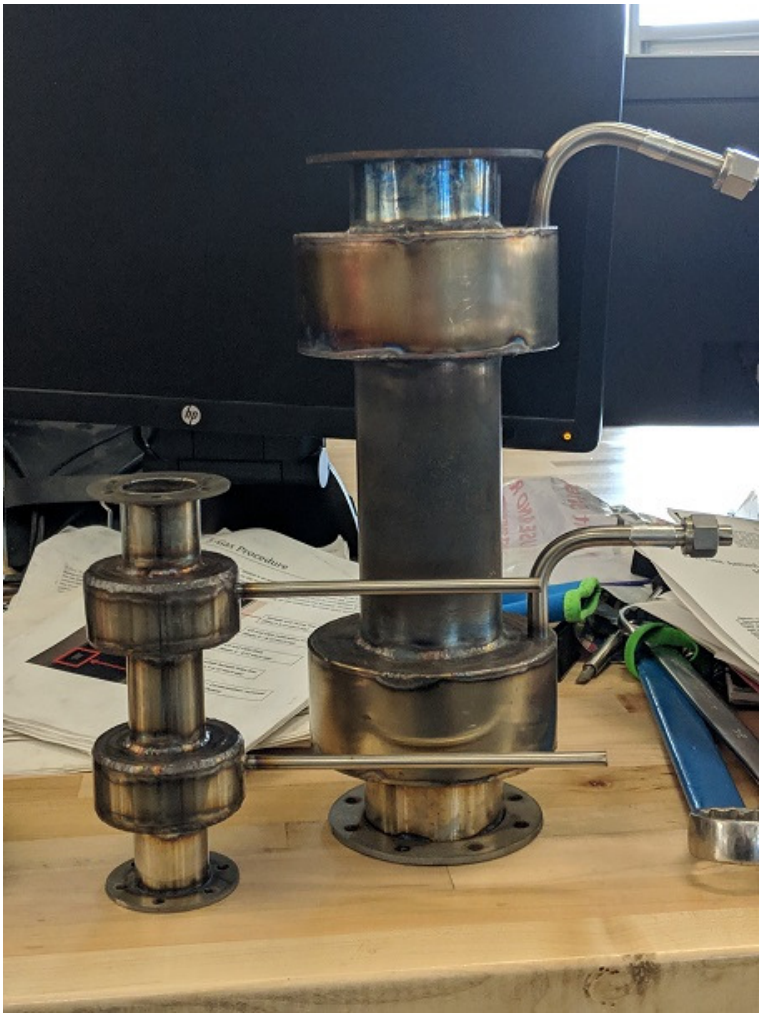

Figure 3.3: Micro mini (left) next to its inspiration, the V3 micro combustor (right).

Chapter 4

Fuel

CSU has a long history conducting research in fecal combustion, all of which suggests that combusting feces is a challenging process [2–4]. However, research showed that the main difficulty was more in the ignition of fecal flakes, due in part to its tendency to get stuck in a smoldering combustion state; this is likely due to differences in donor diet [3]. However, once ignited and steady state is achieved, there was little difference in combustion performance of fecal fuels with other sources [3].

4.1 Fecal Fuel Substitute

While the goal of the micro mini is to be a downsized fecal gasifier, able to size its own fuel by using an auger to grind fuel, it is not available in large quantities for testing, so a substitute was needed. As shown in Table 4.1, pine wood pellets are close in composition to human feces [3]. Testing done in other research has recorded similar values for wood and human feces [21]. Simulant feces created in that study were discussed, but the ease of acquisition and cost for the pine wood made it a better choice for this research.

However, it is not an ideal substitute. The amount of O_2 is double that of feces; this will lead to both lower flame temperatures, which can adversely affect drying of incoming fuel, and a possible skewing of data with regards to equivalence ratio. The ash content of pine is also substantially

Table 4.1: Ultimate analysis for various fuels; all element and ash values are by mass percentage.

Fuel Type	Carbon [%]	Hydrogen [%]	Oxygen [%]	Sulfur [%]	Ash [%]	LHV [kJ/kg]
Canine Feces	36.45	5.00	22.99	0.65	28.52	14114
Human Feces (India)	56.15	6.04	20.32	0.45	12.25	18831
Human Feces (RTI)	48.85	6.63	20.88	0.91	14.83	20854
Wood pellet, Pine	51.28	4.69	40.34	0.15	3.03	19560

less than that of feces. During initial characterization of the micro mini the ash buildup will be minimal, but during fecal fuel testing the ash buildup will be greatly increased and will need to be addressed; the micro combustor used an ash grinder [3].

Pine wood pellet data was obtained from literature [22]. It was assumed the bird litter was of this composition.

Due to the small size of the micro mini, standard sized wood pellets were too large compared to the combustor diameter and would not suffice for testing. A search for commercially available wood pellets in the size needed to fit inside the auger tube yielded crumbled pine bird litter from Petco, shown in Figure 4.1 [23].

Figure 4.1: Petco pine bird litter used for testing.

The average pellet size of the litter ranged from 0.1875 inches to approximately 0.3125 inches in their longest dimension, yet with an oblong shape allowing them to fit inside the auger's flight height. The pellets had an average mass of 0.11 g. This bird litter was used as fuel for all micro mini testing.

For testing purposes, having fuel set to size is ideal, but in future field usage, the energy required to process the fuel down to proper size will need to be addressed. This fuel was conveyed via an auger (Section 5.2). For use in a full toilet system, a machined auger will be able to grind dry feces down to required size.

4.2 Air-Fuel Ratio

The combustion calculator described in Section 2.1.3 also calculates AFR. The code utilized the chemical composition of pine, shown in Table 4.1, and was set to a ϕ of 1 for stoichiometric combustion. The code returned an AFR of 5.94 kg air to every 1 kg of pine pellets. Equation 2.3 was used and returned a value of 5.91 kg air. As the two values were near identical, the code value was accepted and used as the stoichiometric baseline for the test matrices described in Section 7.4.

The code was run again for the Human Feces (India) and Human Feces (RTI) values shown in Table 4.1, returning ratios of 9.17 and 9.02, respectively. These values show that burning feces will require about 50% more air for stoichiometric combustion than the pine wood.

Chapter 5

Fuel Delivery

A continuously operating combustor requires a continuous feed of fuel. Solid fuel feed rate can be difficult to maintain at an exact rate; variability can be expected in combustion performance and missions due to the fuel pieces not being the exact same size or some getting stuck in the fuel chute, only to get knocked loose by more falling fuel that then deposits a double load after a missed cycle.

For this combustor, an auger was chosen for two reasons: one, that it would be relatively easy to control the feed rate of fuel into the combustor by controlling auger rotational speed due to equal spacing of its flights; and two, that an auger powered by a high torque motor would be able to grind dried feces to proper dimensions, which would reduce energy input required to size fuel separately in a final design.

5.1 Fuel Hopper

Due to the small size of the micro mini's wood pellet fuel, a small hopper was all that was required for testing. The 3d printed hopper from the Nano-combustor (Section 1.3) was repurposed to used for the micro mini, shown in Figure 5.1.

5.2 Auger

While the Nano-combustor's fuel hopper was able to be reused, the 3d printed augers it used were designed to convey powder, and as such had a flight height that was too small for pelletized fuel. For the initial benchtop prototype, an auger was acquired that fit within existing acrylic feed tubing. This auger had a 0.625 inch pitch, 0.125 inch flight height, and a shaft diameter of 0.1875 inches. The pitch was larger than desired, as it allowed 2-3 pieces of fuel per revolution, seen in Figure 5.2, but for benchtop prototype testing this was deemed acceptable once fuel feed rates were

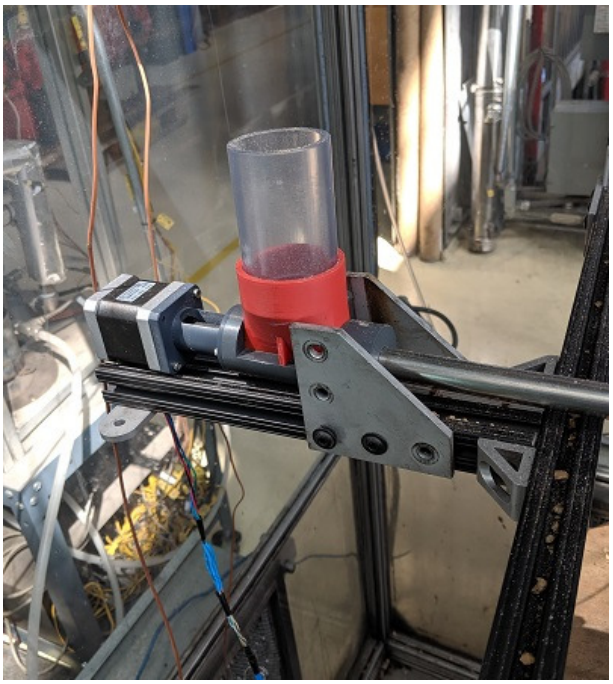

Figure 5.1: Nano-combustor fuel hopper used in this research.

tested and found reasonably consistent. For actual field testing, a more precisely spaced machined auger would be desired to control fuel feed rate to reduce variability of performance.

Figure 5.2: Bird litter fuel next to auger, illustrating size difference.

This auger was used for feeding the fuel into the combustor, as a more expensive auger for grinding feces was not needed for wood pellet testing. The auger was driven by the same Sparkfun stepper motor used by the Nano-combustor (400 steps/rev, 40 N-cm torque, with a NEMA 17 form factor) [24]. The motor was controlled by an Arduino using a potentiometer to control the rotational speed manually shown in Figure 5.3; the original Arduino code was developed by MSR and modified later at CSU to improve performance [4].

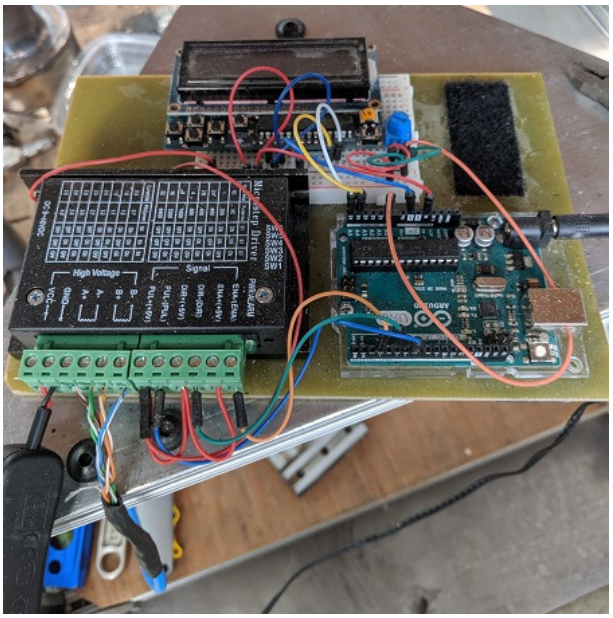

Figure 5.3: Arduino used as motor controller.

The auger was run for 15 minutes using the pine bird litter discussed in Section 4.1 to see if it was feasible for use. One issue that arose was that the bag containing the bird litter had a lot of dust (despite claims on the bag of being 99% dust free) and pieces of fuel that were slightly larger than the auger's flight height, which would agglomerate and jam up the auger. Thereafter, the dust and larger fuel pieces were sifted from the bird litter using a large piece of the fuel grating material prior to loading into the fuel hopper, which solved the problem.

Fuel feed rates at various revolutions per minute (RPM) were measured by running the auger over a scale and repeated three times per rate for an average, shown in Table 5.1. The fuel/hour value was input into the combustion calculator discussed in Section 2.1.3 to determine firepower.

Table 5.1: Fuel feed rates of wood pellet fuel by RPM and expected firepower

Motor RPM	Avg mass, fuel [g]	Avg mass, fuel/hour [g]	Firepower [kW]
5	9.60	192.0	1.012
10	18.07	361.3	1.904
15	24.53	490.7	2.585
20	31.00	620.0	3.267

The returned firepowers were much higher than what the project called for. The Arduino code was set to map the potentiometer to 5 RPM increments; once this was modified by the author down to 1 RPM increments, another test set was run.

Table 5.2: Fuel feed rates of wood pellet fuel by RPM and expected firepower, modified Arduino code

Motor RPM	Avg mass, fuel [g]	Avg mass, fuel/hour [g]	Firepower [kW]
2	3.6	72.0	0.379
3	5.8	116.0	0.611
4	7.7	154.7	0.815

Table 5.2 shows the results of the testing with the modified Arduino code, shown in Appendix B. These firepowers were much more in line with project goals. 1 RPM was tried, but the motor stuttered repeatedly when run at that low a speed. It was suspected the stuttering was caused by a defect with the potentiometer used to control RPM; however, 0.379 kW at 2 RPM was a good benchmark to see how the micro mini functioned at very low firepower. As such, the potentiometer was left as-is.

The results from Tables 5.1 and 5.2 were plotted to generate an RPM vs Firepower curve, shown in Figure 5.4.

The linear fit has an R^2 value of 0.9939, showing a strong correlation and can be used as a general rule of thumb. Ultimately, a motor RPM of 3 was chosen for an expected firepower of 611 W for baseline testing purposes, as that was approximately the level of firepower the micro mini was initially designed for.

5.3 Fuel Chute

A 0.625 inch stainless steel tube was welded onto a piece of 1.18 inch stainless steel tube to act as a fuel chute from the auger down to the combustor. The 8 inch chute was added to keep the acrylic auger housing tube far away from the heat generated by combustion inside the

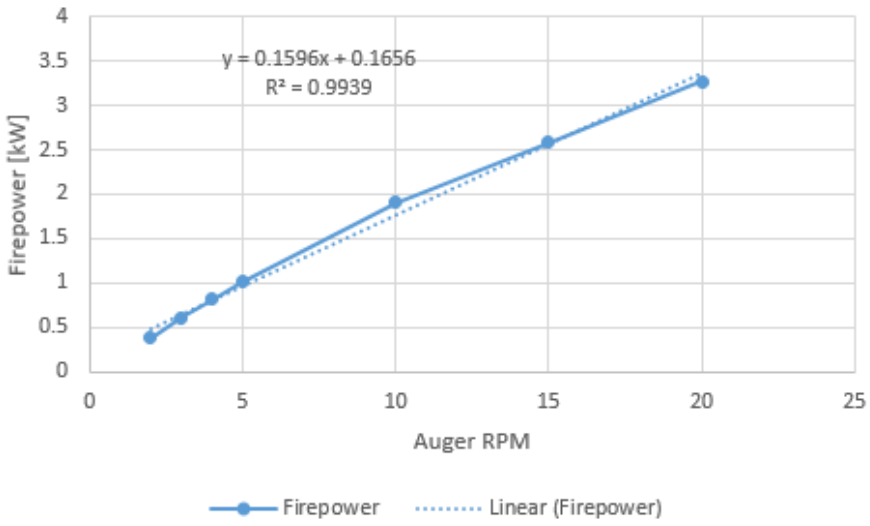

Figure 5.4: Motor RPM versus expected firepower.

main combustor body. The fuel chute assembly was attached to the combustor body using welded flanges as described in Section 3.2.2.

5.4 Integrated System

Figure 5.5 shows the completed micro mini assembly with the addition of motor, auger, and fuel chute.

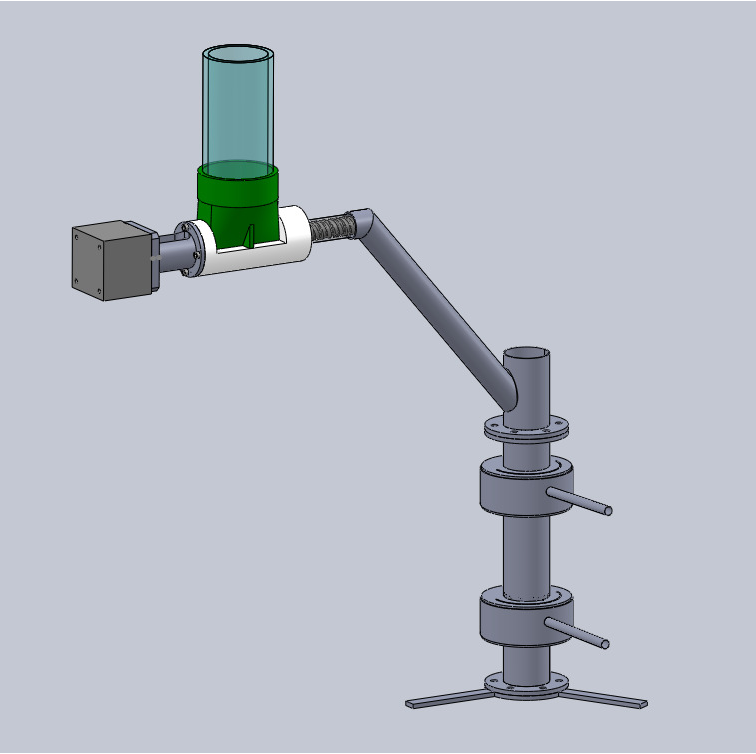

Figure 5.5: Micro mini CAD with fuel delivery system attached.

Chapter 6

Initial Start-up

Upon completion of fabrication and construction of the micro mini and associated assemblies, shown in Figure 6.1, the system was put through an initial test run with no quantitative data collection to see if the system generally functioned as the micro combustor, and to see if any unexpected problems arose from use of repurposed equipment.

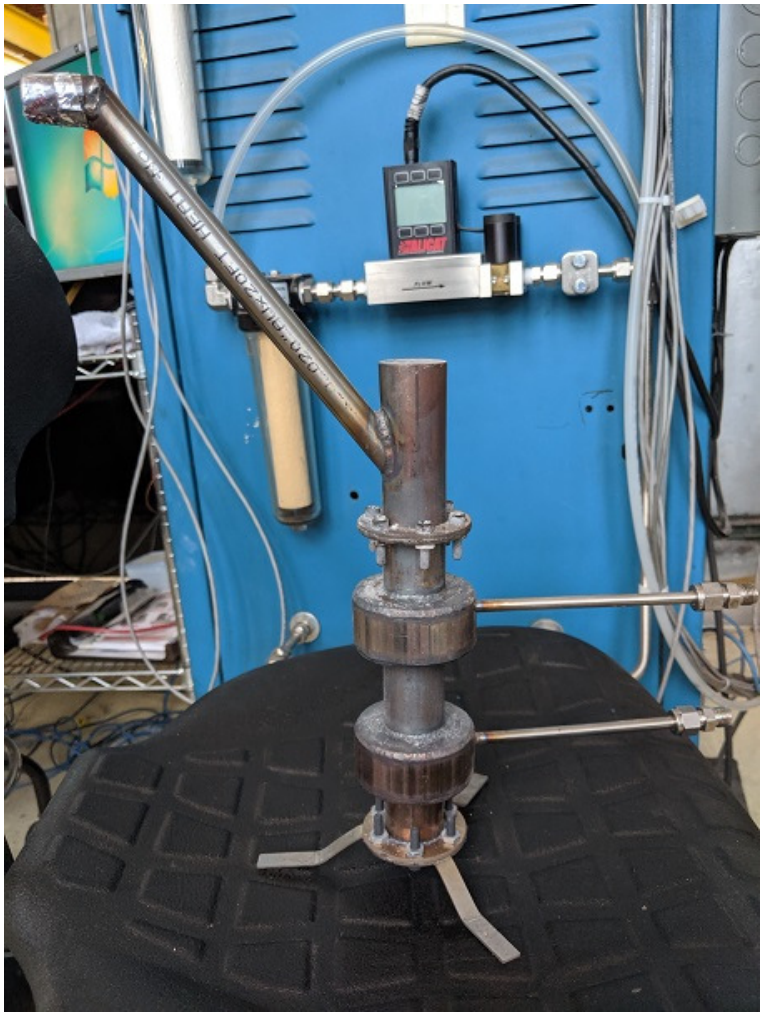

Figure 6.1: Fully assembled micro mini.

The micro mini was mounted on a test stand (Section 7.2.1) and prepared for lightoff, shown in Figure 6.2.

Figure 6.2: Micro mini prepared for testing.

An initial load of 25 g of pine litter was loaded into the combustor, with 15 % weight kerosene (3.75 g) to aid ignition. The air injection mass flow controllers were set 1.7 slpm and 6.8 slpm for primary and secondary air (Section 7.4), respectively, for approximate stoichiometric combustion. Once ignited, the fuel was allowed to burn for 2 minutes to generate a strong flame prior to starting the motor, set to 3 RPM for 116 g/h of fuel for an expected firepower of 611 W, which allowed the auger to continuously feed fuel from the hopper down the fuel chute to the combustor body.

Figure 6.3: Low firepower flame during micro mini initial operation.

This first test ran for one hour prior to shutdown, only requiring the hopper to be refilled every 20 minutes. This proved that the base design was sound and the micro mini functioned as expected with a low firepower flame, such as that shown in Figure 6.3. However, it was noted visually through the acrylic tube that the auger was housed in that fuel had stopped feeding into the auger. Upon disassembly of the hopper assembly, it was discovered two fuel pieces had lodged together at the entrance to the acrylic tube, preventing further fuel transport. This was due to the acrylic tube's wall thickness exceeding the diameter of the hole cut into the hopper.

The acrylic tube was replaced with 304 stainless steel tubing with a wall thickness of 0.02 inches. The thinner walls of the stainless steel tubing combined with a slight widening of the hopper using a drill press were enough that no other fuel seizures occurred during testing.

A second test run was conducted after the auger tube replacement. For this run, the motor RPM was varied from 2 to 5 while varying air flow from stoichiometric values down to a ϕ of 0.5, to explore how the combustor reacted to changing conditions. At high rpm values the flame would occasionally grow very large, an example of which is shown in Figure 6.4, which was approximately 1.2 kW. This run lasted for two hours with no readily apparent stability issues confirming expected operation of the micro mini.

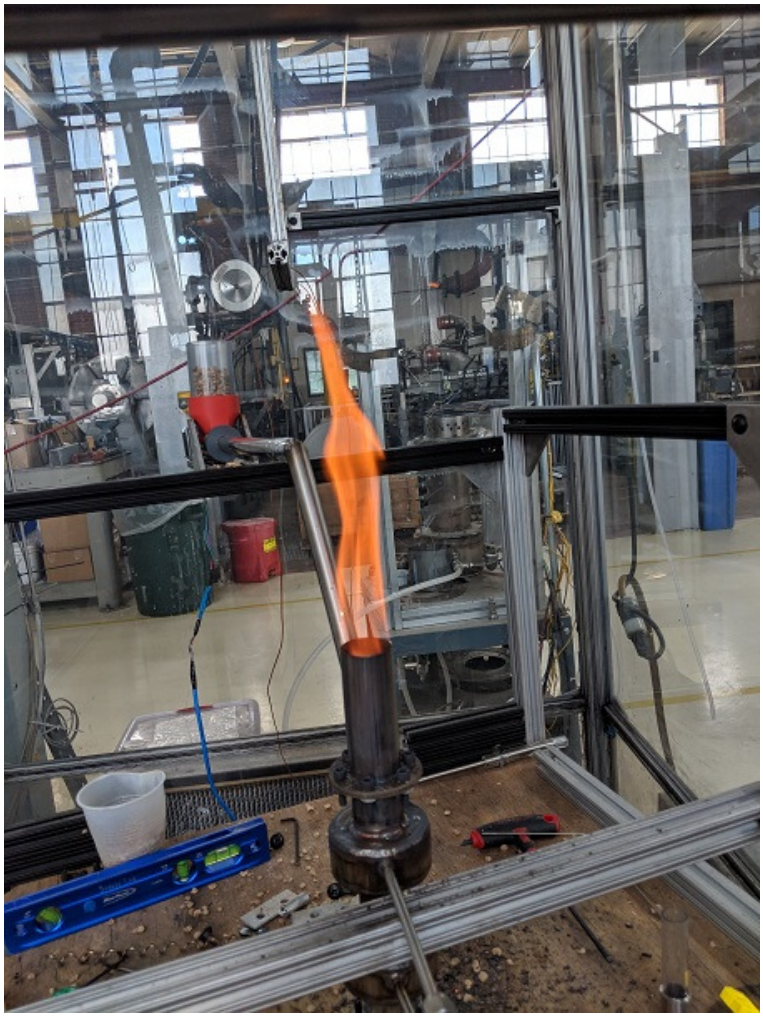

Figure 6.4: High firepower flame during micro mini initial operation.

Chapter 7

Test Procedures

The success of the micro mini's initial characterization test meant that the design was ready for testing. The combustor was setup on its test stand in a large fume hood, shown in Figure 7.1.

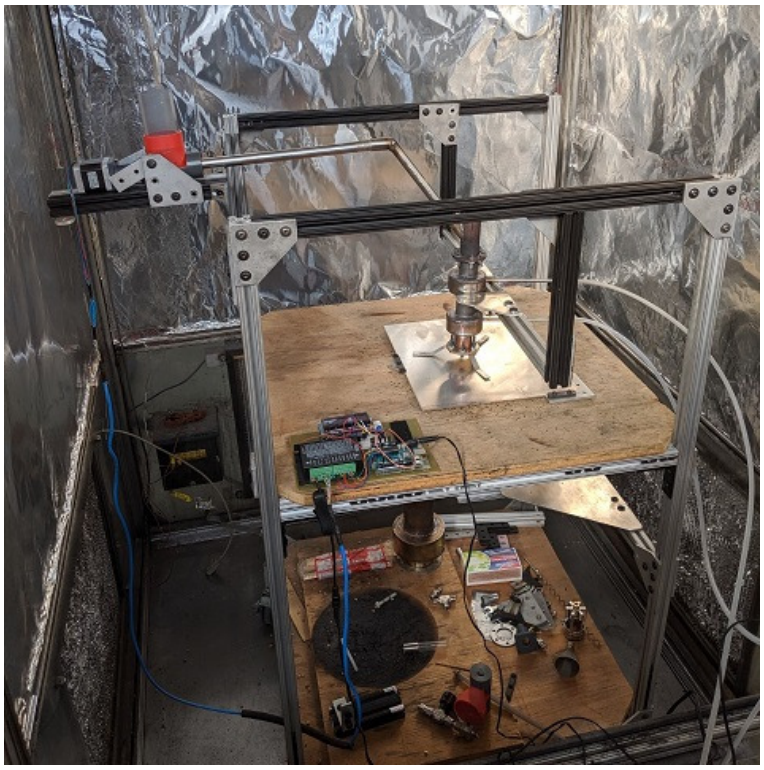

Figure 7.1: Micro mini test setup.

The two main interests for this research were overall stability performance of the combustor and its emissions characteristics for CO_2, CO, and $PM_{2.5}$.

7.1 Combustor Performance

7.1.1 Modified Combustion Efficiency

Modified Combustion Efficiency (MCE) is a method to judge performance of a combustor by calculating the completeness for a combustion process, with an MCE of 1 indicating complete combustion with all carbon in the fuel being converted to carbon dioxide [25]. MCE is calculated as shown in Equation 7.1, with the ΔX representing either carbon monoxide or carbon dioxide after subtracting out background emissions. For this work, MCE was calculated using CO_2 vice CO.

$$\begin{aligned} MCE\ [\%] &= \frac{\Delta CO_2}{\Delta CO_2 + \Delta CO} \\ \Delta X &= X_{\text{emission}} - X_{\text{background}} \end{aligned} \tag{7.1}$$

7.1.2 Emission Factors

The raw CO and CO_2 emissions data are useful in that it's possible to see specific events happening over the duration of a burn, such as a flame out or spike in firepower. Raw data values can also be used in straight numerical comparison between data sets.

Frequently, however, the tests were not able to be directly compared, especially in comparisons between the micro mini and its larger counterparts, as more fuel burned at a higher firepower would necessarily produce more pollutants than a smaller flame with less fuel.

Emission factors were generated for comparisons in these instances. An emission factor is a dimensionless representative value that relates the quantity of a pollutant released with an activity associated with the release of that pollutant [26]. For this research, emission factors were calculated as a ratio of grams of CO/CO_2 produced per gram of fuel burned, as shown in Equation 7.2, with X standing in for either CO or CO_2.

$$EF\left[\frac{g}{g}\right] = \frac{g_{\text{X}}}{g_{\text{fuel}}} \tag{7.2}$$

It should be noted that the Environmental Protection Agency (EPA) uses a unit mass per unit time scale for their published guidelines on allowable emissions. As noted above, this does not account for quantity of fuel burned and as such can skew results towards smaller combustors.

7.2 Testing Apparatus

7.2.1 Test Stand

The full combustor assembly was mounted on a test stand constructed of 80/20 modular aluminum extrusions, shown in Figure 7.1. The test bed had a mount for the fuel hopper, and a platform built underneath the main level to mount the arduino assembly to protect it from any stray solid emissions and dust.

7.2.2 Fume Hood

The micro mini, mounted on the test stand, was placed in a large enclosed fume hood, located in the Engines and Energy Conversion Laboratory (EECL) at CSU's Powerhouse Energy Campus. This fume hood was approximately 4 feet square by 14 feet tall. Exhaust gases from the combustor flowed up through the hood into 5 inch diameter ducting, from which sampling probes fed into both a 5-gas analyzer and a cyclone particle separator, detailed below.

Prior to use in testing, the fume hood sampling probe was calibrated by carbon balance through the use of dry ice. 1 kg of dry ice was placed on a heater to speed sublimination of the dry ice. The CO_2 concentration in the exhaust ducting was recorded and then converted to a mass flow rate, accounting for background CO_2 concentration. This rate was integrated over time for the mass of CO_2 as measured by the 5 gas analyzer and compared to the known value of 1 kg.

7.2.3 Mass Flow Controllers

Three Alicat mass flow controllers were used in the full system. Two were used for primary and secondary air injection on the combustor itself, shown in Figure 7.2, and were run using a

pressurized air line available in the EECL. The third was used to pull air through the cyclone particle separator, and was run using a small pump mounted near the fume hood.

Figure 7.2: Alicat mass flow controllers used for air injection.

Prior to use in testing, all Alicat mass flow controllers had their mass flow verified using an Alicat mass flow tester.

7.2.4 Emissions Measurement

Emissions for CO_2 and CO were recorded using a Siemens 5-Gas analyzer available at the EECL. Raw data for emissions was recorded by LabVIEW^{TM} code used for emissions testing throughout the EECL. Post processing of data was performed through the use of Matlab code developed for use in the Advanced Biomass Combustion Lab. Additional functionality and edits were coded by the author; this code is included in Appendix C.

(a)

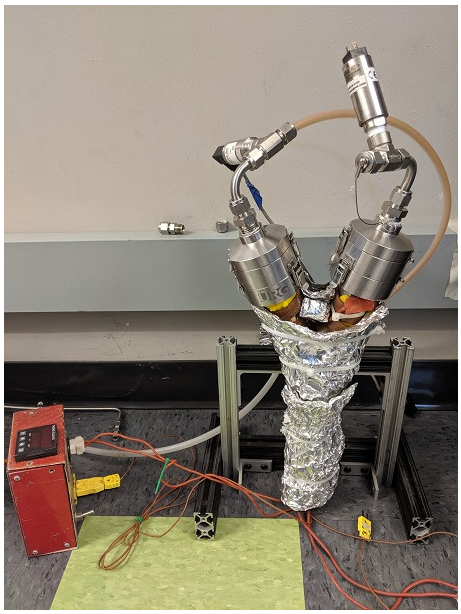

(b)

Figure 7.3: 47 mm Tisch PTFE membrane filter (a), and Cyclone particle separator(b)

7.2.5 Particulate Matter Measurement

The particulate matter was collected on 47 mm Tisch PTFE membrane filters, depicted in Figure 7.3a. These filters were loaded into a URG-2000-30EHS cyclone particle separator sized for $PM_{2.5}$, shown in Figure 7.3b.

The filters were then weighed using a UR3 Robot from Universal Robots, located in the Advanced Aerosols Research Lab located at CSU's Powerhouse Energy Campus. The limit of detection (LOD) and limit of quantification (LOQ) are terms used to describe the smallest amount of PM that can be reliably measured [27]. A limit of detection (LOD), the lowest amount of PM detectable from the absence of blank, of 15 μg was used. A limit of quantification (LOQ), the lowest amount of PM that can not only be detected by reliably measured, of 51 μg was used for these measurements.

7.3 Method

Once the physical hardware was setup, the method for testing was devised, illustrated in Figure 7.4.

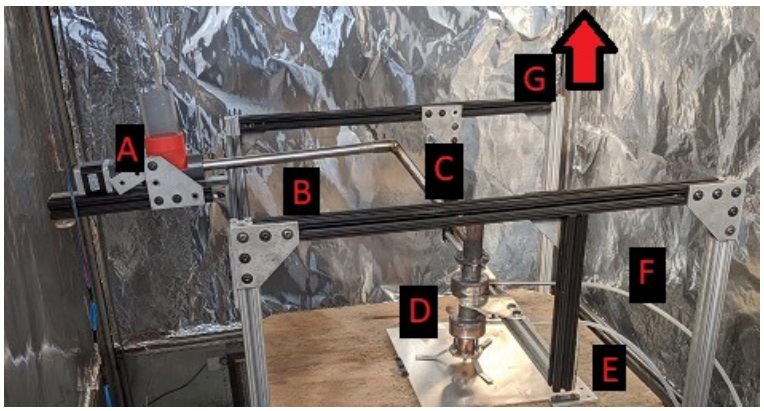

Figure 7.4: Test procedure.

Fuel was loaded into the fuel hopper at (A). The auger then fed the fuel to the fuel chute (B), where it was dropped down (C) onto the fuel grate located in the combustor body (D). Primary air (E) was injected to begin the partial oxidation process, releasing the syngas. The syngas was then combusted at the location of secondary air (F) injection, just below (C). The emissions then left the combustor and went up into the fume hood (G) ducting, where it was then sampled and recorded.

7.4 Performance Testing Matrices

Once testing methods were decided upon, a baseline test matrix was devised, utilizing the standard 1:4 primary to secondary air ratio discussed in Section 2.2.3 and the auger motor set to 3 RPM for an expected firepower of 611 W in accordance with Table 5.2. This baseline test spanned stoichiometric equivalence ratio down to a fuel lean condition of ϕ = 0.5, shown in Table 7.1. Air flow, in standard liters per minute (SLPM), was calculated through the use of Matlab. Primary and secondary air flow was calculated as a percentage of the base air flow measurement.

Based off the results of a study by Tryner *et al* suggesting a 1:3 air ratio may be ideal for gasification, the primary to secondary air ratio was changed to 1:3, keeping firepower steady at

Table 7.1: Test Matrix 1: Varying ϕ, 1:4 primary to secondary air ratio, 611 W firepower.

Equivalence Ratio	AFR	Air Flow [SLPM]	Primary	Secondary
1	5.94	8.62	1.7	6.8
0.9	6.60	9.57	1.9	7.6
0.8	7.42	10.77	2.2	8.6
0.7	8.48	12.31	2.4	9.6
0.6	9.90	14.36	2.8	11.2
0.5	11.88	17.23	3.4	13.6

611 W [28]. This is shown in Table 7.2, again from stoichiometric equivalence ratio down to a fuel lean condition of $\phi = 0.5$.

Table 7.2: Test Matrix 2: Varying ϕ, 1:3 primary to secondary air ratio, 611 W firepower.

Equivalence Ratio	AFR	Air Flow [SLPM]	Primary	Secondary
1	5.94	8.62	2.1	6.3
0.9	6.60	9.57	2.4	7.2
0.8	7.42	10.77	2.7	8.1
0.7	8.48	12.31	3.0	9.0
0.6	9.90	14.36	3.6	10.8
0.5	11.88	17.23	4.3	12.9

The micro mini was designed to operate at approximately 600 W. To study the effects of firepower on combustor performance, the Arduino RPM was changed to vary the fuel feed rate, sweeping the firepower from calculated values of 380 W to 1 kW.

As preliminary results from test matrices 1 and 2 indicated a low of carbon monoxide emissions at an equivalence ratio of 0.6, a shorter sweep of ϕ was conducted for test matrix 3, from 0.7 to 0.5, as shown in Table 7.3.

To investigate the performance of the micro mini as a standard batch fed updraft gasifier and to compare emissions from batch fed versus continuous fuel feeding, the micro mini was detached from the auger and run with an initial batch of 20g fuel, with 15% weight (3g) of kerosene to light quickly. The kerosene enabled the batch fed tests to reach steady state faster to allow for more

Table 7.3: Test Matrix 3: Varying ϕ, 1:4 primary to secondary air ratio, varying firepower.

Equivalence Ratio	RPM	Firepower [kW]	AFR	Air Flow [SLPM]	Primary	Secondary
0.7	2	0.379	8.48	7.64	1.5	6.0
0.6	2	0.379	9.90	8.91	1.8	7.2
0.5	2	0.379	11.88	10.7	2.1	8.4
0.7	4	0.815	8.48	16.41	3.3	13.2
0.6	4	0.815	9.90	19.15	3.8	15.2
0.5	4	0.815	11.88	22.97	4.6	18.4
0.7	5	1.012	8.48	20.37	4.0	16.0
0.6	5	1.012	9.90	23.77	4.8	19.2
0.5	5	1.012	11.88	28.52	5.7	22.8

accurate comparison. The batch fed tests were conducted using the same test matrix detailed in Table 7.1.

7.5 Emissions Testing

The raw CO and CO_2 data obtained in Section 7.4 was used to compare outputs of the micro mini at different air ratios, firepower, and operating modes. This data was also used to compare the CO and CO_2 outputs of the micro mini to the V2, V3, and monofold micro combustors (Section 1.2.1). Unfortunately, the Nano-combustor's development was focused on proof of concept, not characterization, and as such there is no data to compare to.

A repeat of Table 7.1 was conducted for 2.5 μm Particulate Matter ($PM_{2.5}$) emissions, both in continuous feed and batch fed operational modes.

Chapter 8

Combustor Emissions: CO and CO_2

8.1 Modified Combustion Efficiency

MCE for the micro mini combustor was above 99% during steady state operations at all air flow rates and firepowers. This is comparable to the micro combustor the micro mini descended from. Both far exceed the 67-80% measured using the original downdraft combustor [3].

An example of MCE for the micro mini, run with continuous fuel feed at an equivalence ratio of 0.6, can be seen in Figure 8.1.

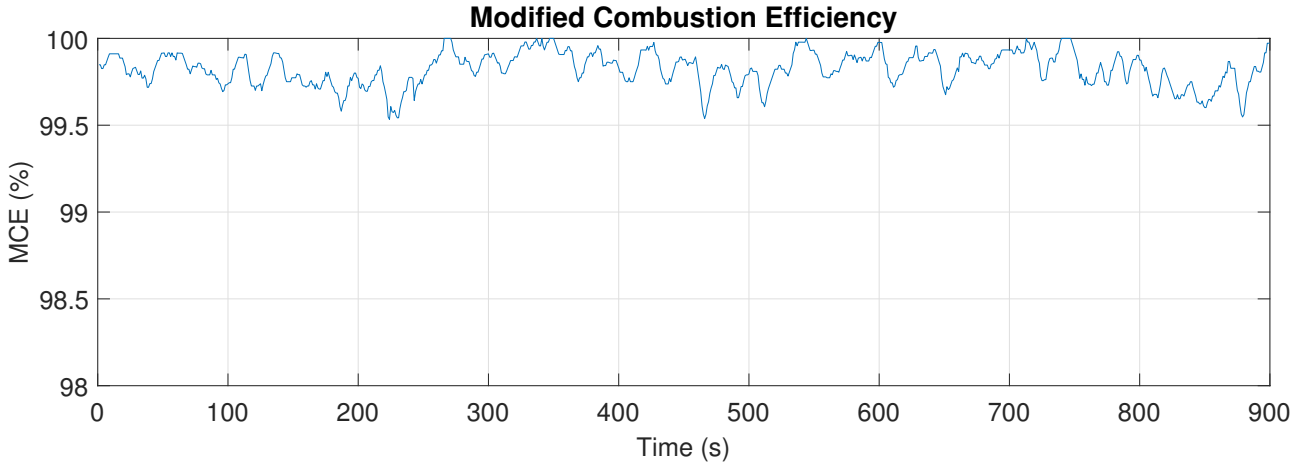

Figure 8.1: MCE for micro mini combustor at ϕ=0.6

The only times MCE was below this value was during initial ignition or when the combustor stopped burning syngas and started burning the fuel bed (usually due to fuel addition mishaps), as shown in Figure 8.2 with CO and CO_2 levels. CO_2 levels began to decline before the sharp spike in CO due to the flame out event, but quickly returned to steady state values upon relight.

The char combustion at the fuel bed only had primary air for oxidation, since secondary air was downstream of the combustion process. This meant the flame was operating in a fuel rich condition, which produces more CO, and this CO was not oxidized in a secondary combustion

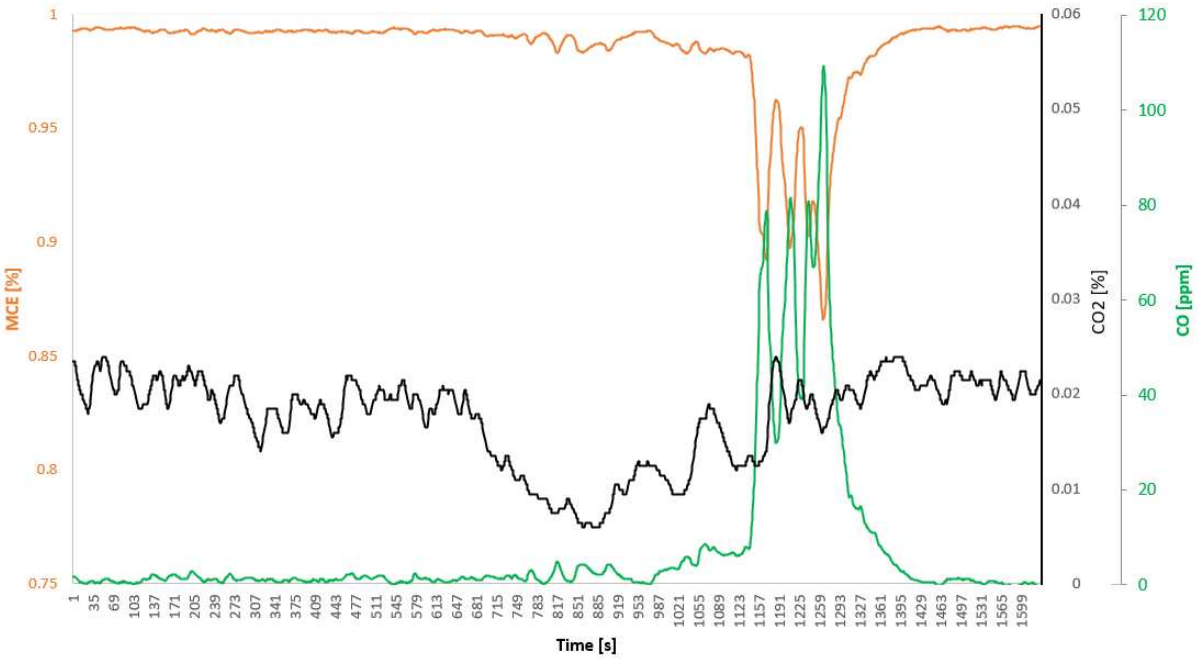

Figure 8.2: MCE for micro mini combustor at ϕ=0.5 with a halt in fuel addition.

zone, as discussed in Section 2.2. In this example, the auger flight had come loose from the auger shaft, preventing fuel addition, which caused the syngas to stop being produced in large enough quantities to sustain flame.

8.2 Baseline Emissions

Figure 8.3 shows CO emissions obtained, in parts-per-million (ppm), for the micro mini operating at baseline conditions (1:4 primary to secondary air ratio, 611 W firepower), with varying equivalence ratio. With the exception of some transient events, values of CO were low and typically below 5 ppm.

Figure 8.4 shows CO_2 emissions obtained, by percentage, for the micro mini operating at baseline conditions and varying equivalence ratio. All equivalence ratios produced similar results for CO_2 emissions.

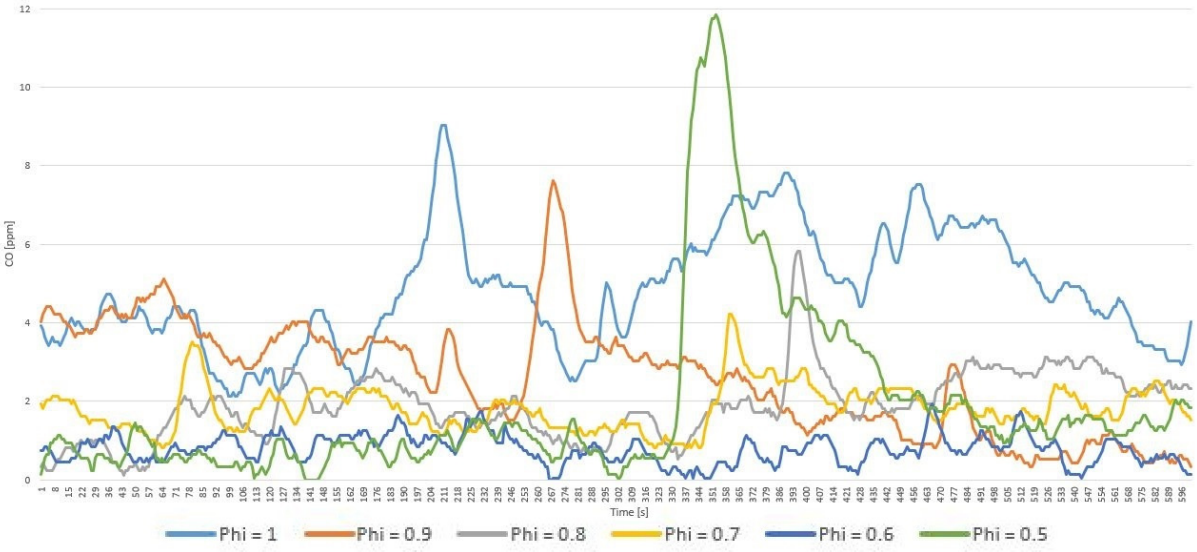

Figure 8.3: Carbon monoxide emissions from baseline configuration.

Figures 8.3 and 8.4, while useful in some instances, do not lend themselves to easy comparison, and in fact are very confusing. Based on the discussion in Section 7.1.2, emissions factors were calculated for baseline conditions for ease of comparison between the baseline and modified conditions, as per Equation 7.2.

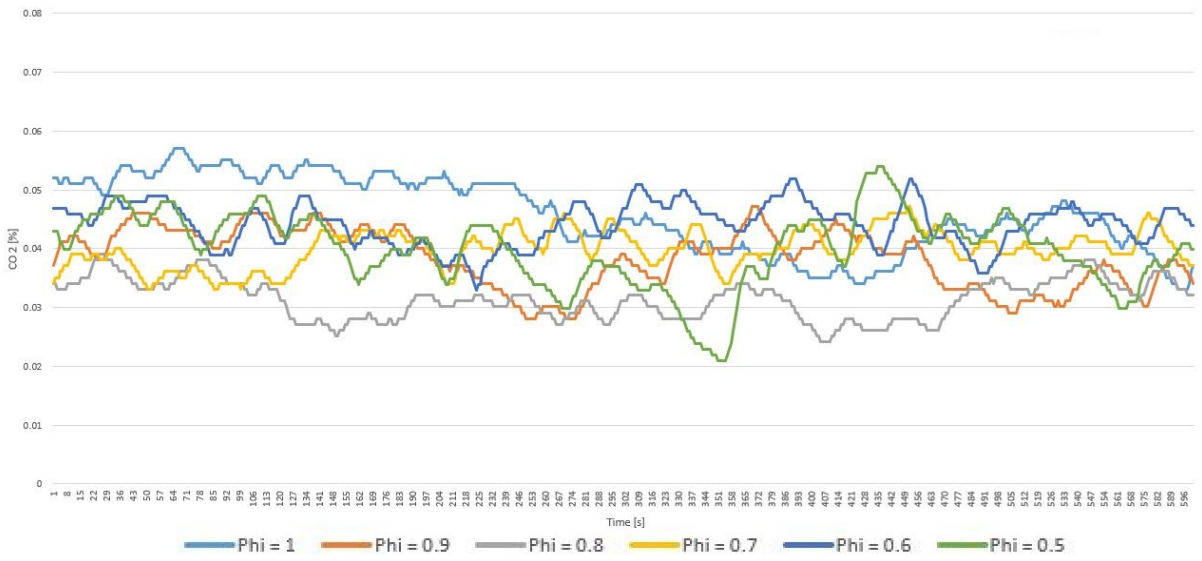

Figure 8.4: Carbon dioxide emissions from baseline configuration.

These emissions factors are shown numerically in Table 8.1 and graphically in Figure 8.5. The data shown is for 1:4 primary to secondary air, 611 W, with varied equivalence ratio.

Table 8.1: Calculated emissions factors [$g_{emission}/g_{fuel}$], baseline conditions.

Phi	EF_{CO}	EF_{CO_2}
1	0.01005	1.8562
0.9	0.008	1.8620
0.8	0.0071	1.8480
0.7	0.00565	1.8592
0.6	0.0021	1.8652
0.5	0.0056	1.8597

Figure 8.5 also shows one standard deviation from baseline tests conducted. An equivalence ratio of 0.7 was the most consistent between tests, while $\phi = 0.8$ included a data set that had a very short flame out condition before it self-reignited via spark.

An equivalence ratio of $\phi = 0.6$ proved to have the lowest carbon monoxide emissions for baseline conditions.

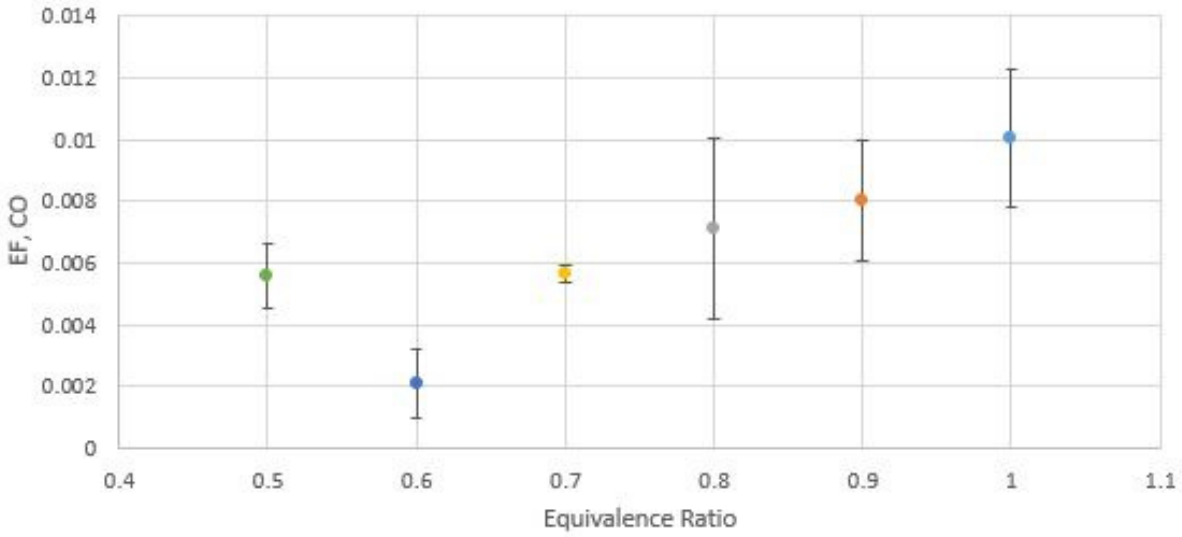

Figure 8.5: Micro mini baseline emission factors, $\pm$ one standard deviation.

8.3 Change in Air Ratio

After baseline data were collected, the air flow ratio between primary and secondary air injection was changed from 1:4 to 1:3 and the test matrix from Table 7.2 was conducted. Table 8.2 shows the emission factors.

Table 8.2: Calculated emissions factors [$g_{emission}/g_{fuel}$], 1:3 air ratio

Phi	EF_{CO}	EF_{CO_2}
1	0.0105	1.852
0.9	0.0097	1.8532
0.8	0.0058	1.8627
0.7	0.0047	1.8642
0.6	0.0021	1.8652
0.5	0.0039	1.8623

The 1:3 air ratio performed extremely similar to the baseline air ratio of 1:4. As with baseline, the new air ratio had a low of CO emissions at ϕ = 0.6. This is graphically shown in Figure 8.6. The 1:4 baseline data is slightly offset to the left of the 1:3 data to improve readability.

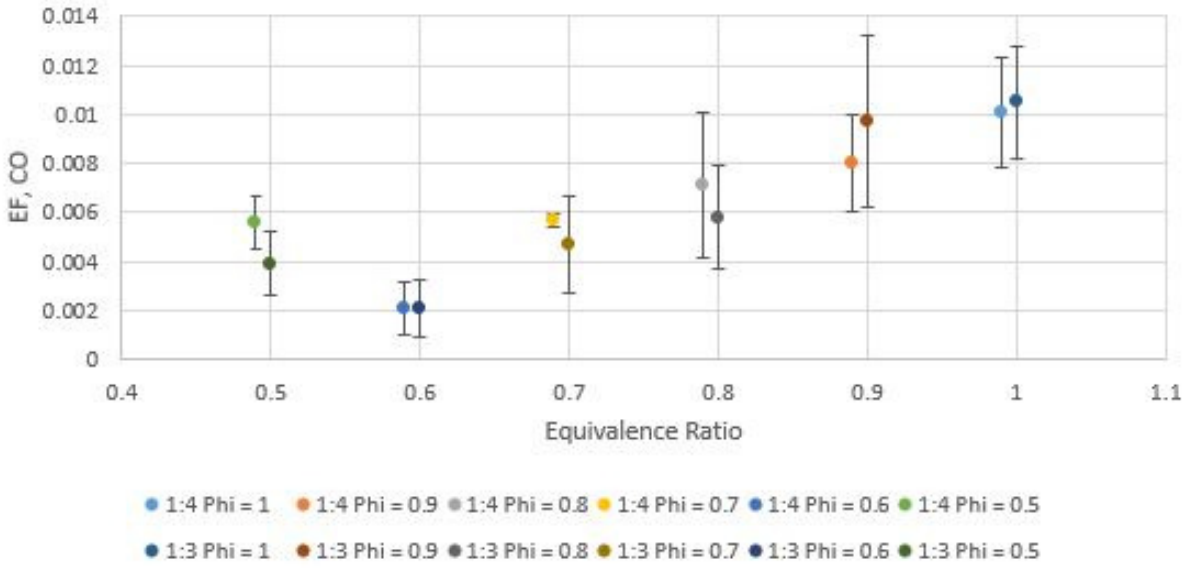

Figure 8.6: Emission factors comparison of 1:4 and 1:3 primary to secondary air ratios.

8.4 Change in Firepower

Air ratio was returned to 1:4 for the firepower sweep testing. Changes were made in motor rpm ranging from 2 to 5 for expected firepowers from 380 W to 1 kW, as calculated from Matlab code and shown in Tables 5.1 and 5.2. Table 8.3 shows calculated carbon monoxide emission factors, while Table 8.4 shows carbon dioxide emission factors.

Table 8.3: Calculated emission factors [$g_{emission}/g_{fuel}$] by RPM, 1:4 air, carbon monoxide

Phi	2 [rpm]	3 [rpm]	4 [rpm]	5 [rpm]
0.7	0.0102	0.0059	0.0101	0.0152
0.6	0.0083	0.0021	0.0059	0.0091
0.5	0.0134	0.0056	0.0099	0.0115

As was with the two different primary to secondary air ratios, a lowest CO emissions were experienced at an equivalence ratio of 0.6. The emission factors are plotted graphically in Figure 8.7.

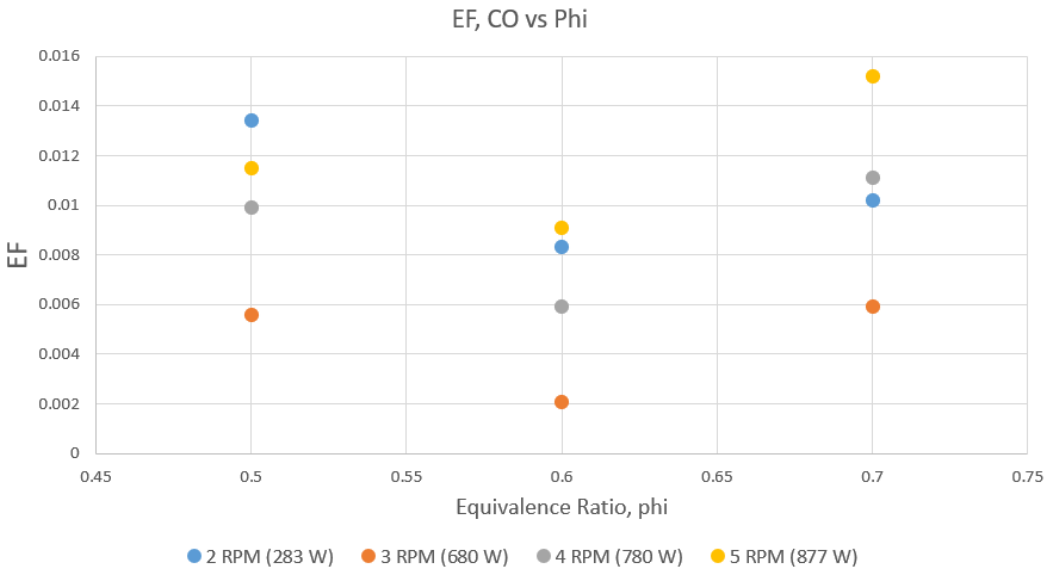

Figure 8.7: Emission factors comparison of varied RPM.

This suggests that as the combustion process was increasingly leaned out, the combustor was approaching the lower limit of flammability, discussed in Section 2.1.4; flame propagation may become impossible at lower equivalence ratios, especially in the 2 rpm case.

Table 8.4: Calculated emission factors [$g_{emission}/g_{fuel}$] by RPM, 1:4 air, carbon dioxide

Phi	2 [rpm]	3 [rpm]	4 [rpm]	5 [rpm]
0.7	1.8525	1.8592	1.8525	1.8445
0.6	1.8554	1.8652	1.8591	1.8542
0.5	1.8473	1.8597	1.8529	1.8504

Expected vs Actual Firepower

Table 8.5: $\dot{m}$ calculated firepower vs Matlab calculated firepower

Matlab firepower [kW]				
Phi	2 [rpm]	3 [rpm]	4 [rpm]	5 [rpm]
All	0.379	0.611	0.815	1.019
Measured firepower [kW]				
Phi	2 [rpm]	3 [rpm]	4 [rpm]	5 [rpm]
0.7	0.25	0.63	0.74	0.85
0.6	0.31	0.74	0.82	0.89
0.5	0.29	0.67	0.78	0.89

As shown in Table 8.5, measured values of firepower from tests show generally lower-than-expected values, except for 3 motor rpm, which was slightly above. This may be due to the micro mini being designed for that firepower.

8.5 Change in Operational Mode

Table 8.6 shows calculated emission factors for batch fed operation. EF_{full} are the values of the batch fed run from ignition to the fuel being mostly consumed. $EF_{burning}$ are the values of the batch fed run from ignition until the LabVIEW^{TM} code showed declining CO_2 levels, which indicated the flame was going out; this occurred at approximately 10 minutes for all tests. This was done to more directly compare batch fed operation versus continuous feed.

Table 8.6: Calculated emissions factors [$g_{emission}/g_{fuel}$], batch fed

Phi	$EF_{CO,full}$	$EF_{CO_2,full}$	$EF_{CO,burning}$	$EF_{CO_2,burning}$
1	0.0419	1.8026	0.0057	1.8595
0.9	0.0501	1.7898	0.0222	1.8335
0.8	0.0636	1.7685	0.0528	1.7856
0.7	0.0573	1.7784	0.0054	1.8599
0.6	0.0336	1.8157	0.0059	1.8592
0.5	0.0262	1.8274	0.0075	1.8566

When analyzing a full burn cycle of startup-steady state-char combustion, clearly continuous fuel feeding has much better emission factors than the batch fed operation. However, if the final phase of burning char (seen when the CO_2 levels fall) is removed, the emission factors are reduced to levels that are comparable to continuous fuel feed emission factors. Table 8.7 and Figure 8.8 show a comparison of a full batch burn, syngas burn only, and continuous feed emission factors.

Table 8.7: Comparison of full run batch, burning only batch, and continuous feed emission factors

Phi	Batch EF_{full}	Batch $EF_{burning}$	Continuous
0.7	0.0573	0.0054	0.00565
0.6	0.0336	0.0059	0.0021
0.5	0.0262	0.0075	0.0056

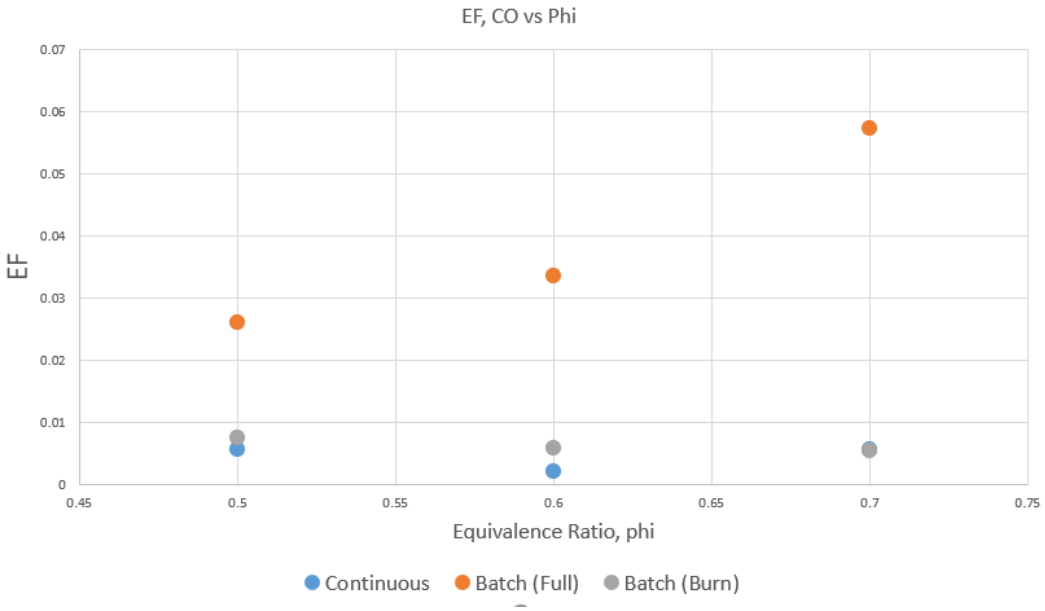

Figure 8.8: Emission factors comparison, graph of Table 8.7.

8.6 Comparison Against Larger Combustors

The micro mini emissions were compared against the V2 and V3 micro combustor, as well as the micro monofold combustor. Emission factors were used exclusively for comparison due to the size difference between the larger combustors and the micro mini.

Table 8.8: Comparison of CO emission factors between combustors.

Name	EF,CO	EF,CO2
V2 Micro	0.138	1.8128
V3 Micro	0.0078	1.8221
Micro Monofold	0.0082	1.8188
Micro Mini, Phi = 1	0.0101	1.8526
Micro Mini, Phi = 0.6	0.0021	1.8652

The V3 micro combustor was an improvement over the V2, while the monofold was a different configuration of the V3. The larger combustors were run at at 5% excess air. The micro mini, being a smaller descendant of the V3, has a higher emission factor for CO than the V3 at stoichiometric value, but as was seen in Table 8.5, quickly outpeforms the V3 with decreasing equivalence ratio. This is especially noticeable at ϕ = 0.6 for the micro mini.

Figure 8.9 shows a bar graph representation of Table 8.8. The micro mini depends on a lean equivalence ratio to exceed the CO emission factors of the large combustors.

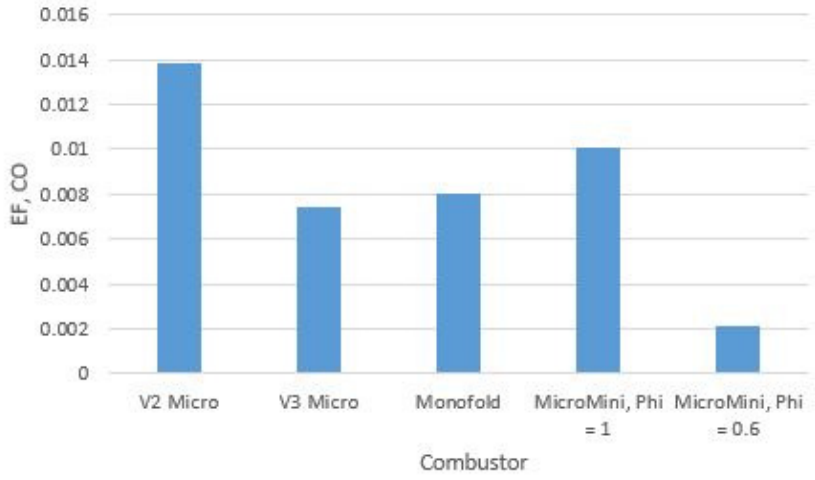

Figure 8.9: CO emission factor comparison between combustors.

8.7 Consolidated CO Emissions Factors

Table 8.9: Calculated emission factors [$g_{emission}/g_{fuel}$]

3 RPM, 1:4 air ratio	Phi	CO	CO_2
	0.7	0.00565	1.8592
	0.6	0.0021	1.8652
	0.5	0.0056	1.8597
3 RPM, 1:3 air ratio	Phi	CO	CO_2
	0.7	0.0047	1.8642
	0.6	0.0021	1.8652
	0.5	0.0039	1.8623
2 RPM, 1:4 air ratio	Phi	CO	CO_2
	0.7	0.0102	1.8525
	0.6	0.0083	1.8554
	0.5	0.0134	1.8473
4 RPM, 1:4 air ratio	Phi	CO	CO_2
	0.7	0.0101	1.8525
	0.6	0.0059	1.8591
	0.5	0.0099	1.8529
5 RPM, 1:4 air ratio	Phi	CO	CO_2
	0.7	0.0152	1.8445
	0.6	0.0091	1.8542
	0.5	0.0115	1.8504
Batch (full), 1:4 air ratio	Phi	CO	CO_2
	0.7	0.0573	1.7784
	0.6	0.0336	1.8157
	0.5	0.0262	1.8274
Batch (burning), 1:4 air ratio	Phi	CO	CO_2
	0.7	0.0054	1.8599
	0.6	0.0059	1.8592
	0.5	0.0075	1.8566

Chapter 9

Combustor Emissions: Particulate Matter

As stated in Section 7.2.5, an LOD of 15 μg and a LOQ of 51 μg was used for particulate matter measurements. All particulate matter data was above the LOD, and all but 4 (noted below) were above LOQ.

The duct from the fume hood being 4.86 inches in inner diameter and the sampling probe having a diameter of 0.257 inches in inner diameter meant only a portion of the exhaust was being sampled. To account for this, Equation 9.1 was applied to account for the differences in area.

$$PM_{2.5,\text{actual}} = PM_{2.5,\text{measured}} \frac{Area_{\text{duct}}}{Area_{\text{probe}}} \tag{9.1}$$

9.1 Continuous Feed Emissions

Table 9.3 shows the $PM_{2.5}$ on the filter as measured by the UR3 robot and after Equation 9.1 was applied, as well as calculated emissions factors. The micro mini was operating at 1:4 air flow ratio, 611 W, with varying air ratio for these test runs.

Table 9.1: $PM_{2.5}$ amount, in μg, by equivalence ratio for continuous fuel feed

Phi	$PM_{2.5}$ [μg]	PM_{actual} [μg]	PM_{rate} [g_{PM}/g_{fuel}]
1	56	19906.80	0.000729
0.9	94	33615.08	0.001425
0.8	25	8940.18	0.000389
0.7	57	20383.61	0.001054
0.6	24	8453.37	0.000370

It is clear that the amount of $PM_{2.5}$ produced by the micro mini is very small, with two of the test runs below LOQ. Emission factors likewise are very small.

9.2 Batch Fed Emissions

Table 9.2 shows the $PM_{2.5}$ on the filter as measured by the UR3 robot and after Equation 9.1 was applied, as well as emission rates in g/hr. Air ratio was set to 1:4. The batch of fuel was 20 g of fuel, with 15% wt kerosene (3 g) to ease ignition.

The Alicat pulling air through the cyclone particle separator was turned off when the LabVIEW^{TM} code showed declining CO_2 levels, which indicated the flame was going out; this occurred at approximately 10 minutes for all equivalence ratios.

This was done for ease of comparison against continuous feed operation; once the syngas flame went out, smoke would necessarily emit in large quantities from the combustor, completely throwing the balance in favor of continuous feed operation.

Table 9.2: $PM_{2.5}$ amount, in μg, by equivalence ratio for batch fed operation

Phi	$PM_{2.5}$ [μg]	PM_{actual} [μg]	PM_{rate} [g_{PM}/g_{fuel}]
1	52	18714.78	0.000890
0.9	169	60435.62	0.000293
0.8	786	281198.48	0.012301
0.7	37	13350.67	0.000543
0.6	29	10370.61	0.000423

The micro mini operating in batch fed operational mode continues to produce very little in the form of PM. The slightly elevated value at ϕ = 0.9 was due to the syngas flame going out momentarily before relighting from a spark.

The much higher value at ϕ = 0.8 is from the flame going completely out, with a lot of smoke being emitted while attempts at relighting were made. While the data point should be omitted due to not falling within test parameters that require steady state conditions, it in fact gives confidence in the rest of the obtained values as proper operation clearly produces small values of PM.

The elevated value at ϕ = 0.5 is due to a similar operator error in not turning off the Alicat pulling exhaust samples into the cyclone at the same time as at other equivalence ratios.

In the remaining tests, PM values are similar to continuous feed operation.

9.3 Comparison to Micro Combustor

As noted in Section 7.1.2, the EPA uses a mass per unit time scale for their guidelines. All of the particulate matter data generated for the micro combustor was reported in those terms. As such, in order to compare the micro mini to the micro combustor in terms of PM emissions, the micro combustor data was back calculated to allow for emission factor comparison. As the micro combustor was run as a continuous feed device, the micro mini's continuous data will be used for comparison purposes.

Table 9.3: $PM_{2.5}$ amount, in μg, by equivalence ratio for continuous fuel feed

Phi	$PM_{2.5}$ [μg]	PM_{actual} [μg]	PM_{rate} [g_{PM}/g_{fuel}]
Micro Mini			
1	56	19906.80	0.000729
0.9	94	33615.08	0.001425
0.8	25	8940.18	0.000389
0.7	57	20383.61	0.001054
0.6	24	8453.37	0.000370
Micro Combustor			
Wood	210	75000.0	0.001500
Dog Feces	1435	513000.0	0.005130
Human Feces	3561	1273500.0	0.015269

The only direct comparison is the micro combustor burning wood, which was recorded at an average firepower of 1.77 kW. The micro combustor operated at stoichiometric values, so comparing that to the micro mini's stoichimetric value show double the emission factor.

Comparison between standard pellet stoves, the micro combustor, and the micro using EPA standards of mass per unit time can be seen in Appendix D, Figures D.1 and D.2.

Chapter 10

Conclusions

10.1 Summary of Findings

The micro mini has proven to be an efficient, continuous burning low firepower combustor with low carbon monoxide and particulate matter emissions.

The combustor operates well at firepowers from 250 W to 890 W, with highest stability achieved at 611 W.

The combustor functions at peak condition at an equivalence ratio of 0.6 across all tested firepowers, two different primary to secondary air ratios, and two different operating modes. This is clearly shown by the minimum of CO emissions at this equivalence ratio in all data.

The micro mini, therefore, would work well in a redesigned toilet system such as that the micro combustor was used in, but on a considerably smaller scale. Further, the transient emissions penalties the larger system suffers from are avoided by the continuous operation of the micro mini, providing benefits to human health.

10.2 Suggestions for Future Work

Feces as Fuel

The micro mini was designed as a combustor to incinerate feces, but all characterization was done using pine wood as fuel for the reasons described in Section 4.1. However, as was done with the micro combustor, the micro mini needs to be run using dried feces as its fuel to ensure it can fulfill the primary objective it was designed to perform.

Investigation of Drying Ability

Feces is roughly 74.8% wet material, meaning it needs to be dried thoroughly before it can be effectively used as a fuel for a combustor. The micro mini should be able to utilize heat from the

combustion process to dry incoming fuel. Tests should be conducted to see if the incoming fuel can be dried effectively at an equivalence ratio of 0.6 (being the best in terms of low emissions), or if combustion temperature needs to be higher to effectively dry the fuel, or if residence time of fuel must be increased to allow for ample drying.

Investigation of LFL vs Minimum Fuel Addition

The micro mini was tested at 6 different equivalence ratios, from stoichiometric to a phi of 0.5. As was shown in Section 8.4, it is the author's opinion that at very lean conditions the combustor may be approaching the lower limit of flammability. Another possibility is that as the primary air rate is increased, the dry fuel consumption is also increased, and that there is a minimum mass flow rate (and thus a minimum achievable firepower) required for operation.

Dry fuel consumption rate was not explicitly verified. Carbon balance was the primary method to measure fuel addition against carbon monoxide and carbon dioxide emissions.

However, during batch fed operation tests, 20g of initial fuel load was consumed to char in approximately 10 minutes across all equivalence ratios, suggesting a standard 2 g/min consumption rate. Operating in continuous fuel feed at 3 motor rpm feeds approximately 2 g/min, which would mean no fuel buildup in the combustor. However, this stands in contrast to previous work, which showed a linear relationship in primary air to dry fuel consumption [19].

It would be interesting to see what happens at lower equivalence ratios, and to see if each firepower tested has a minimum equivalence ratio or mass flow rate the combustor will operate at, or if the linear relationship described above either does not apply or applies but at a much slower rate to a combustor of this scale.

Multiple Combustors

Larger combustors are sometimes too large for the task at hand. The micro combustor, for instance, is designed to only operate for up to 12 hours a day, and has large emission values at startup and shutdown.

This was, in fact, one of the reasons for designing a smaller combustor: to operate continuously and avoid these large emission penalties. It has been proven in this work that the micro mini emits less pollutants than the larger combustors it was based off and compared to. As such, when a task is called for that requires the larger firepower of a bigger combustor, it might be more efficient to operate several smaller combustors in an array vice one larger combustor.

Micro combustor equivalence ratio study

The micro mini is based off the micro combustor previously developed at CSU. However, the micro combustor was only run at an equivalence ratio of $\backsim$0.95, while data from this work clearly shows that the optimal air for this style of combustor is 0.6.

It would be interesting to rerun some operational tests using the larger micro combustor at much leaner conditions to see if 0.6 is the optimal ratio for the combustor style in general, or if the optimal equivalence ratio depends on the size of the combustor itself.

Bibliography

[1] RTI International. Reinventing the Toilet. https://www.rti.org/impact/reinventing-toilet. [Online; accessed 04-October-2019].

[2] Nathan Loveldi. Development of a Solid Human Waste Semigasifier Burner for Use in Developing Countries. Master's thesis, Department of Mechanical Engineering, Colorado State University, Fort Collins, CO, 2014.

[3] Maxwell Flagge. Development of a Combustion System for Fecal Materials. Master's thesis, Department of Mechanical Engineering, Colorado State University, Fort Collins, CO, 2017.

[4] Kyle Greer. Development of a Low-Firepower Biomass Dust Combustor. Master's thesis, Department of Mechanical Engineering, Colorado State University, Fort Collins, CO, 2018.

[5] P. Yadav et al. Performance analysis of the constructed updraft biomass gasifier for three different biomass fuels. *International Journal of Modern Engineering Research*, 3(4):2056–2061, 2013.

[6] World Health Organization. Sanitation. http://www.who.int/news-room/fact-sheets/detail/sanitation. [Online; accessed 20-August-2019].

[7] Wolf J. Bartram J. Clasen T. Cumming O. Freeman M. C. âĂę Johnston R. PrÃijss-UstÃijn, A. Burden of disease from inadequate water, sanitation and hygiene for selected adverse health outcomes: An updated analysis with a focus on low- and middle-income countries. *International Journal of Hygience and Environmental Health*, 222:765–777, 2019.

[8] Bill & Melinda Gates Foundation. Water, Sanitation & Hygiene: Reinvent the Toilet Challenge. https://docs.gatesfoundation.org/Documents/Fact_Sheet_Reinvent_the_Toilet_Challenge.pdf. [Online; accessed 29-September-2019].

[9] Parker A. Jefferson B. Rose, C. and E. Cartmell. The characterization of feces and urine: a review of the literature to inform advanced treatment technology. *Crit. Rev. Environ. Sci. Technol.*, 45:1827–1879, 2015.

[10] Daniel Wilson Cristina Ceballos Thomas Kirchstetter Jonathan Slack Larry Dale Randy Maddalena, Melissa Lunden. Quantifying Stove Emissions Related to Different Use Patterns for the Silver-mini (Small Turkish) Space Heating Stove. Technical report, Ernest Orlando Lawrence Berkeley National Laboratory, 2012.

[11] UN Women. Ending violence against women: creating safe public spaces. unwomen.org/en/what-we-do/ending-violence-against-women/creating-safe-public-spaces, note = [Online; accessed 18-April-2020].

[12] Kelly Banta; Linden Klein; Ian Norris; Kyle Greer; John Mizia; and Mars Rayno. Design and Engineering Assessment of a Powderized Biomass Microburner. Technical report, Mountain Safety Research and Colorado State University, 2019.

[13] A. Adamson. *Physical Chemistry of Surfaces*. John Wiley Sons, 6th edition, 1997.

[14] Stephen R. Turns. *An Introduction to Combustion: Concepts & Applications*. New York: McGraw-Hill, 3rd edition, 2012.

[15] C. Higman and M. van der Burgt. *Gasification*. Oxford: Gulf Professional, 2009.

[16] Department of Energy. Syngas composition. /urlhttps://www.netl.doe.gov/research/coal/energy-systems/gasification/gasifipedia/syngas-composition. [Online; accessed 21-April-2020].

[17] S. Chandak. Thermo-chemical conversion technologies - biomass gasification. 2013.

[18] A. Bhavanam and R. Sastry. Biomass gasification processes in downdraft fixed bed reactors: A review. *International Journal of Chemical Engineering and Applications*, 2(6):425–433, 2011.

[19] Jessica Tryner. *Combustion Phenomena in Biomass Gasifier Cookstoves*. PhD thesis, Department of Mechanical Engineering, Colorado State University, Fort Collins, CO, 2016.

[20] B.A. Rabee. The effect of inverse diffusion flame burner-diameter on flame characteristics and emissions. *Energy*, 160:1201–1207, 2018.

[21] T. et al Onabanjo. An experimental investigation of the combustion performance of human faeces. *Fuel (London)*, 184:780–791, 2016.

[22] TNO - Innovation for Life. https://phyllis.nl/Biomass/View/1786. [Online; accessed 07-August-2019].

[23] Planet Petco Crumbled Pine Bird Litter, 10 lbs. https://www.petco.com/shop/en/petcostore/product/planet-petco-crumbled-pine-bird-litter-10-lbs-2318021.

[24] Sparkfun Stepper Motor, 400 steps/rev, 12VDC, 1.7A, 48 N*cm Torque. https://www.sparkfun.com/products/10846.

[25] N.L. Briggs et al. "method to calculate modified combustion efficiency and its uncertainty supplement to: Particulate matter, ozone, and nitrogen species in aged wildfire plumes observed at the mount bachelor observatory".

[26] Environmental Protection Agency. Basic Information of Air Emissions Factors and Quantification. (2019, July 25). https://www.epa.gov/air-emissions-factors-and-quantification/basic-information-air-emissions-factors-and-quantification. [Online; accessed 16-October-2019].

[27] David Armbruster and Terry Pry. Limit of blank, limit of detection and limit of quantification. *The Clinical Biochemist*, 2008.

[28] Jessica Tryner; James Tillotson; Marc Baumgardner; Jeffrey Mohr; Morgan DeFoort; and Anthony Marchese. The effects of air flow rates, secondary air inlet geometry, fuel type,

and operating mode on the performance of gasifier cookstoves. *Environmental Science & Technology*, 50:9754–9763, 2016.

Appendix A

Matlab Code - Combustion Calculator

```
clear; clc;
%% Inputs

% phi = 1;
% m_dot_fuel = 500/3600/1000; %kg/s
% T = 800+273.15; LHV = 0;
%
% % Input mass fractions
% mf.C = 50.62;
% mf.H = 6.78;
% mf.N = 4.79;
% mf.O = 21.9;
% mf.S = 0.99;
% mf.ash = 14.92;

[mf, phi, m_dot_fuel, T_exh, LHV, mass_based, T_amb, P_amb] = func_GUI_inputs;




%% Constants
P_FC = (12.3/14.6959)*101325; %Pa, taken to be pressure in Fort Collins
Ru = 8315; % J/kmol-k
%Molar Masses, kg/kmol
MW.C = 12.011;
MW.H = 1.0079;
MW.O = 15.999;
```

```
MW.N = 14.0067;
MW.S = 32.065;
MW.air = 28.9645;
MW.CO2 = MW.C + 2*MW.O;
MW.H2O = MW.H*2 + MW.O;
MW.N2 = 2*MW.N;
MW.SO2 = MW.S + 2*MW.O;
MW.O2 = 2*MW.O;
r_air = Ru / MW.air;
lambda = 1/phi;
%%SLPM based on alicat stp (25c and 14.696 psi)
P_stp= 101325.353;
T_stp = 273.15;

rho_air = (P_amb) / (r_air * (T_amb)); % CSU (12.3psi/20C) (kg/m^3)


%% Convert Mass-based to moles
if mass_based == 1
    % Convert to ashless mass fraction
    Y.ashless = mf.C + mf.H + mf.N + mf.O + mf.S;
    Y.C = mf.C/Y.ashless;
    Y.H = mf.H/Y.ashless;
    Y.O = mf.O/Y.ashless;
    Y.N = mf.N/Y.ashless;
    Y.S = mf.S/Y.ashless;

    % Convert to molar fuel chemistry CaHbOcNdSe

    MW.fuel = 1/(Y.C/MW.C + Y.H/MW.H + Y.O/MW.O + Y.N/MW.N + Y.S/MW.S); % ...
       ashless fuel, kg/kmol, EQ 2.12b

    % mole fractions of fuel constituents, eq 2.11b
```

```
    a = Y.C*MW.fuel/MW.C;
    b = Y.H*MW.fuel/MW.H;
    c = Y.O*MW.fuel/MW.O;
    d = Y.N*MW.fuel/MW.N;
    e = Y.S*MW.fuel/MW.S;

else % if inputs were already molar-based
    a = mf.C;
    b = mf.H;
    c = mf.O;
    d = mf.N;
    e = mf.S;

    MW.fuel = a*MW.C + b*MW.H + c*MW.O + d*MW.N + e*MW.S;
end

%% Combustion Equation: CaHbOcNdSe + A(O2 +3.76N2) --> aCO2 + b/2H20 + ...
    (d/2 + 3.76A)N2 + eSO2 + fO2

A_s = a + b/4 + e - c/2; %Stoich 'A'
A = A_s./phi; % Eq 2.33: N_air_act = N_air_stoich*phi
f = A - A_s; % moles excess air
N_prod = a + b/2 + (d/2 + 3.76*A) + e + f;

%% Flow Rate Calcs
AF_stoic = 4.76 * A_s * MW.air/MW.fuel; %EQ 2.32
AF_act = AF_stoic./phi; % Fuel:Air Flowrate

m_dot_ashless = (1 - mf.ash/100)*m_dot_fuel;

m_dot_air = AF_act * m_dot_ashless; % kg/s
Q_air = (m_dot_air * 60 * 1000) / (rho_air); %l/m
m_dot_exhaust = m_dot_air + m_dot_ashless; %kg/s
```

```
%% Molar Fractions Exhaust
mol_frac.co2 = a./N_prod;
mol_frac.h2o = (b/2)./N_prod;
mol_frac.n2 = (d/2 + 3.76.*A)./N_prod;
mol_frac.so2 = e./N_prod;
mol_frac.o2 = f./N_prod;

%% Exhaust Ideal Gas, Flowrate Calc
P_i = [P_amb*mol_frac.co2, P_amb*mol_frac.h2o, P_amb*mol_frac.n2, ...
    P_amb*mol_frac.so2, P_amb*mol_frac.o2]; %Pa
for idx = 1:numel(T_exh)
    rho_i = (1./(T_exh(idx).*Ru)).*[P_i(1).*MW.CO2, P_i(2).*MW.H2O, ...
        P_i(3).*MW.N2, P_i(4).*MW.SO2, P_i(5).*MW.O2];  %kg/m3
    rho_tot(idx) = sum(rho_i); %kg/m3
end

Q_exhaust = 60000.*m_dot_exhaust./rho_tot; %L/min
SLPM_ex = Q_exhaust.*(P_amb/P_stp).*((T_stp)/T_exh); %changed to reflect ...
    alicat STP

%% Print Chemical Rxn
fprintf('\n\nRESULT:\n\nphi = %.2f: ', phi)
if phi > 1
    fprintf('Fuel Lean')
else
    fprintf('Stoichiometric')
end
fprintf('\n\n      C %.2f H %.2f O %.2f N %.3f S %.4f + %.2f(O2+3.76N2) ...
    --> %.2f CO2 + %.2f H2O + %.2f N2 + %.4f SO2', a,b,c,d,e,A,  ...
    a,b/2,d/2+3.76*A, e);

if phi > 1
```

```
        fprintf(' + %.2f O2 ',  f)
end

fprintf(' \n\n T_stp:  %.2f C \n', T_stp-273.15)
fprintf(' P_stp: %.2f psia \n\n', P_stp*0.000145038)
fprintf(' T_amb: %.2f C \n', T_amb - 273.15)
fprintf(' P_amb: %.2f psia \n\n', P_amb*0.000145038)
fprintf(' M_dot solid fuel: %.2f g/hr\n\n', m_dot_fuel*3600*1000)
fprintf(' Exhaust Temp: %.2f C\n', T_exh - 273.15)
fprintf(' Exhaust Flowrate: %.2f lpm (T_exh, P_amb)\n', Q_exhaust)
fprintf(' Exhaust Flowrate: %.2f slpm (T_stp , P_stp)\n', SLPM_ex)

if LHV ≠ 0
    firepower = m_dot_ashless*LHV;
    fprintf(' Firepower: %.3f kW\n', firepower)
    fprintf(' m_dot_air: %.2f g/hr\n', m_dot_air * 3600 *1000)
    fprintf(' Q_air: %.2f lpm (T_amb, P_amb)\n', Q_air)
    fprintf(' Q_air: %.2f slpm (T_stp , P_stp)\n', Q_air * 273.15/T_amb * ...
       P_amb/101325)
    fprintf(' m_dot_fuel: %.2f g/hr\n', m_dot_fuel * 3600 *1000)
    fprintf(' Mass Air Fuel Ratio: %.2f g_air/g_fuel\n', AF_act)
    fprintf(' energy to heat air to exhaust temp: %.2f kw\n', m_dot_air * ...
       1.025 * (T_exh - T_amb))

end

fprintf('\n\n')
```

Appendix B

Arduino Code - Auger Control

```
/*FOR USE WITH ADAFRUIT DISPLAY SHIELD WITH MICROSTEP DRIVER AND ...
   POTENTIOMETER.
 * MICROSTEP DRIVER NEEDS SEPARATE POWER SUPPLY (E.G. 12V)
 * 5V ACROSS POTENTIOMETER.  ADJUSTABLE PIN TO A0.
 *
 * ORIGINALLY BY LINDEN KLEIN
 * MSR
 * UPDATED BY KYLE GREER, CSU
 * Modified RPM scaling by Mars Rayno, CSU
 */

// include the library code:
#include <Wire.h>
#include <Adafruit_RGBLCDShield.h>
#include <utility/Adafruit_MCP23017.h>
#include <math.h>

// These #defines make it easy to set the backlight color
#define OFF 0x0
#define RED 0x1
#define YELLOW 0x3
#define GREEN 0x2
#define TEAL 0x6
#define BLUE 0x4
#define VIOLET 0x5
#define WHITE 0x7
```

```
Adafruit_RGBLCDShield lcd = Adafruit_RGBLCDShield();

int PUL = 7;            //define Pulse pin
int DIR = 6;            //define Direction pin
int ENA = 3;            //define Enable Pin
float microstep = 4.0;  //make sure this matches what's on the driver dip ...
   switch.
int StepPerRev = 400;   //using a 400 step per rev stepper motor
int maxRPM = 100;       // let minRPM = 0. **** MaxRPM is 100RPMs for 4 ...
   microsteps. 200RPM for 2 microsteps
int RPM;
int pot;

unsigned int DELAY;
unsigned int dwell;

void setup() {
  pinMode (PUL, OUTPUT);
  pinMode (DIR, OUTPUT);
  pinMode (ENA, OUTPUT);

  Serial.begin(9600);      //if using the serial monitor

 //RPM & potentiometer setup
  pot = map(analogRead(A0), 0, 1020, 0, maxRPM/1);        // map ...
     potentiometer so RPMs step in increments of 1. Map to 1020 instead ...
     of 1023 because max potentiometer is unstable between 1020&1023 so ...
     maxRPM is unstable if max pot = 1023.
  RPM = pot * maxRPM / (maxRPM/1);
  DELAY = round(6E7 / 2 / StepPerRev / microstep / RPM);  // DELAY is the ...
     time for a half pulse cycle (high or low). DELAY will be an ...
     microsecond integer, so rounding error will occur. If no ROUND fxn, ...
     then it will just drop the decimal, so use ROUND.
```

```
 //LCD Screen Setup
  lcd.begin(16, 2);
  lcd.setCursor(0, 0);
  lcd.print(microstep);
  lcd.print(" microsteps");
  lcd.setCursor(0, 1);
  lcd.print("RPM=");
  lcd.print(RPM);
  delay(3000);
  lcd.clear();
  lcd.setCursor(0, 0);
  lcd.print("RPM");
  lcd.setCursor(0, 1);
  lcd.print(RPM);
  lcd.print(" FP: ");
  lcd.print(RPM*175);

  digitalWrite(DIR, HIGH);  //change this to run in the other direction
  digitalWrite(ENA, HIGH); //start spinning motor
}

void loop() {

// dwell times the microseconds it takes to read the analog and check the ...
    if statement.
dwell = micros();
pot = map(analogRead(A0), 0, 1020, 0, maxRPM/1);

  // check if the potentiometer was turned. If so, update LCD
  if (RPM != pot * maxRPM / (maxRPM/1) ) {
    RPM = pot * maxRPM / (maxRPM/1);
    DELAY = round(6E7 / 2 / StepPerRev / microstep / RPM);
```

```
    //update LCD
    lcd.setCursor(0, 1);
    lcd.print(RPM);
    lcd.print(" FP: ");
    lcd.print(RPM*175);
  }

 // Advance motor one full pulses
  digitalWrite(PUL, HIGH);
  dwell = micros() - dwell;
  delayMicroseconds(DELAY-dwell);   // subtract the time for the analog ...
      read from the DELAY time.

  digitalWrite(PUL, LOW);
  delayMicroseconds(DELAY);
}
```

Appendix C

Matlab Code - Emissions

```
%% Five Gas Data Processing to produce Fire Power and MCE
%% Initial Code by Max Flagge; edits by Mars Rayno

%% Instruction
% # using the icon on HOME tab, IMPORT DATA
% # Find the excel file in your data
% # Pop-up window will appear and select the two column of CO2 and CO
% # Do NOT select the first row which are the title in excel
% # Import emission as a matrix (first column is CO2 and second is CO)
% # rename the emission data to 'emission'
% # save matrix as RAW.mat wherever in the same location as this program
% # Check and adjust constant
% # RUN / PUBLISH

%% ASSUMPTIONS:
% # ideal gas
% # assuming that the data will start as ambient condition for the first
% 30s
% # ambient pressure is obtained from daily weather data in fort collins
% # blower speed depends on test, so make sure it is correct, and
% displacement per volume is as indicated
% # substracting the concentration values from ambient condition to give us
% actual produced concentration
clc
clear
load('RAW.mat')
%specify font_size
```

```
font_size = 15;


%% Emission RAW

%CO2 and CO in volume concentration
CO2_ind = emission(:,1)./100 ;
CO_ind = emission (:,2)./1000000;


%% CONSTANT (CHECK)
V_blower = 1320; %RPM
Q_blower_per_Rev = 0.004813;%m^3/rev
Q_blower = V_blower * Q_blower_per_Rev / 60 ; % m^3/s
R = 8.314 ; % J / mol K
Cp_H2O = 4.186 ; % (J/g c)
MW_CO = 28.01 ; %g/mole
MW_CO2 = 44 ; %g/mole
MW_C = 12.01; %g/mole
MW_air = 28.97 ;
Carbon_percent_fuel = 0.51 ;
LHV = 19.56; %kJ/g

%% AMBIENT CONSTANT (CHECK)
time_amb = 30; %s
P_amb = 84557.3 ; %Pa
T_amb = 304.04; %K
CO2_amb = 0.000411; %percent/100
CO_amb = 0.00000496; %ppm/1,000,000


%% Densities (kg/m^3)
%PV = NRT
```

```
% m/V = P * MW / R / T(K)

rho_CO = P_amb * MW_CO / (R *(T_amb)) / 1000; %kg/g conversion%
rho_CO2 = P_amb * MW_CO2 / (R *(T_amb)) / 1000;
rho_air = P_amb * MW_air / (R *(T_amb)) / 1000;

%% MCE calculation

CO_act = CO_ind - CO_amb;
CO2_act = CO2_ind - CO2_amb;

for zz = 1: length(CO_act)
    if CO_act(zz)<0
        CO_act(zz) = 0;
    end
end
for zz = 1: length(CO2_act)
    if CO2_act(zz)<0
        CO2_act(zz) = 0;
    end
end
CO_true = emission(:,2)-(CO_amb*1000000);
CO2_true = emission(:,1)-(CO2_amb*100);
for zz = 1: length(CO_true)
    if CO_true(zz)<0
        CO_true(zz) = 0;
    end
end
for zz = 1: length(CO2_true)
    if CO2_true(zz)<0
        CO2_true(zz) = 0;
    end
end
```

```
%CO plot
figure (1)
plot(CO_true);
set(gca,'FontSize',font_size);
xlabel('Time (s)','FontSize',font_size);
ylabel('CO(ppm)','FontSize',font_size);
title ('CO vs time');
grid on;

%CO2 plot
figure (2)
plot(CO2_true);
set(gca,'FontSize',font_size);
xlabel('Time (s)','FontSize',font_size);
ylabel('CO2(%)','FontSize',font_size);
title ('CO2 vs time');
grid on;

%MCE is in percent

MCE = CO2_act./(CO_act+CO2_act) .*100;
AnotNaN = ¬isnan(MCE);

figure (3)
plot(MCE);
set(gca,'FontSize',font_size);
xlabel('Time (s)','FontSize',font_size);
ylabel('MCE (%)','FontSize',font_size);
title ('Modified Combustion Efficiency');
ylim ([50 100]);
grid on;

%% FIRE POWER calculation
```

```
CO_mdot = CO_act .* rho_CO ./rho_air .* Q_blower *1000 ; % g/s
CO2_mdot = CO2_act .* rho_CO2 ./rho_air .* Q_blower *1000 ; % g/s
C_mdot = (CO_mdot .* MW_C ./ MW_CO) + (CO2_mdot .* MW_C ./ MW_CO2); %g/s
fuel_mdot = C_mdot ./ Carbon_percent_fuel; % g/s
fire_power = fuel_mdot * LHV ;

figure (4)
plot(fire_power);
set(gca,'FontSize',font_size);
xlabel('Time (s)','FontSize',font_size);
ylabel('Fire Power (kW)','FontSize',font_size);
title ('Fire Power');
grid on;

%% CO percent
figure (5)
CO_perc = (emission(:,2))/10000;
plot(CO_perc);
set(gca,'FontSize',font_size);
xlabel('Time (s)','FontSize',font_size);
ylabel('CO(%)','FontSize',font_size);
title ('CO vs time');
grid on;

%% fuel_mdot
figure(6)
plot(C_mdot)
set(gca,'FontSize',font_size);
xlabel('Time (s)','FontSize',font_size);
ylabel('Carbon (g/s)','FontSize',font_size);
title ('Carbon Mdot');
grid on;
```

```
X = sum(CO_mdot);
Y = sum(fuel_mdot);
Z = sum(CO2_mdot);
C = sum(C_mdot);
D = Y * Carbon_percent_fuel;
EFCO = X/Y;
EFCO2 = Z/Y;
AVGFR = mean(fuel_mdot);
AVGFP = mean(fire_power);
AVGMCE = mean(AnotNaN);
AVGCO = mean(CO_true);
AVGCO2 = mean(CO2_true);
EFSTD = CO_mdot./fuel_mdot;
EFSTD2 = CO2_mdot./fuel_mdot;
AAA = std(EFSTD);
BBB = std(EFSTD2);
fprintf(' \n\n Total CO: %.2f g, Total CO2: %.2f g, Total Carbon: %.2f g ...
   \n', X, Z, C)
fprintf(' \n\n Avg CO: %.2f ppm, Avg CO2: %.4f percent \n', AVGCO, AVGCO2)
fprintf(' \n\n EFCO: %.4f,  EFCO2: %.4f, Avg MCE: %.4f \n', EFCO, EFCO2, ...
   AVGMCE)
fprintf(' \n\n Total Fuel: %.2f g, Avg Fuel Rate: %.4f g/s, Avg FP: %.2f ...
   kW \n', Y, AVGFR, AVGFP)
fprintf(' \n\n StdDev CO: %.4f , StdDev CO2: %.4f \n', AAA, BBB)
```

Appendix D

PM Emissions Using EPA Standards

Figure D.1 shows the micro combustor and micro mini compared against a wide variety of pellet stoves, along with current EPA regulation of 75 mg/min and the proposed 33 mg/min regulation due to take effect summer 2020.

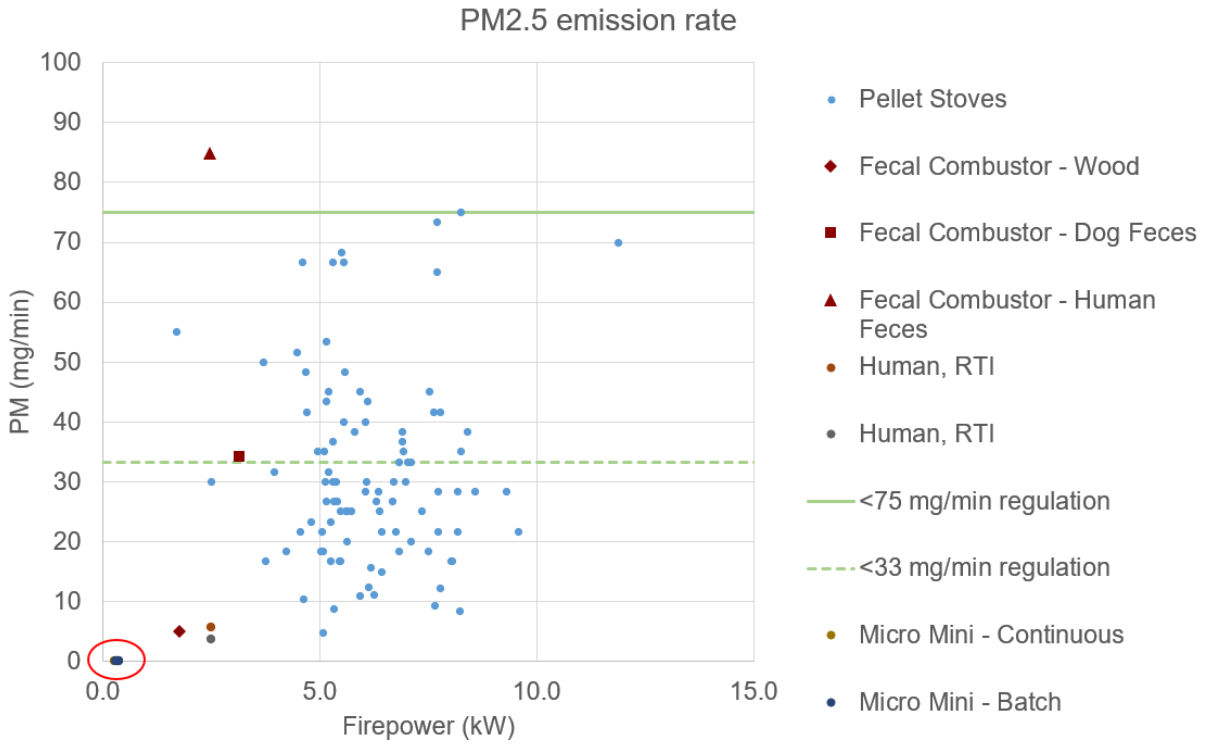

Figure D.1: Particulate Matter data using EPA standards, multiple combustors.

The small red circle in the bottom corner shows the micro mini's data. This clearly shows that using mass per unit time as a standard skews data sharply towards preferring smaller combustors as opposed to larger ones.

As it is impossible to see the actual data, Figure D.2 shows the same data, but zoomed into the bottom corner.

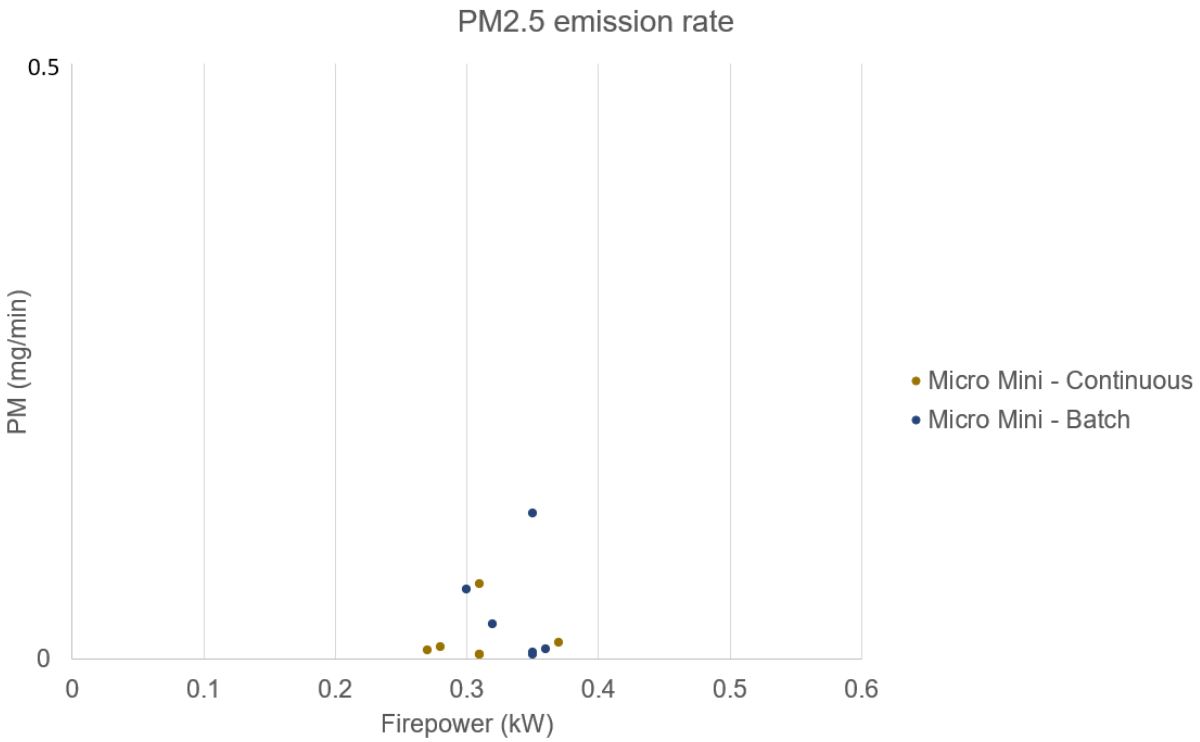

Figure D.2: Particulate Matter data using EPA standards, micro mini only.